R-05-86

Bedrock transport properties

Preliminary site description Forsmark area – version 1.2

Johan Byegård, Eva Gustavsson, Geosigma AB

Eva-Lena Tullborg, Terralogica AB

Jan-Olof Selroos, Svensk Kärnbränslehantering AB

December 2006

Svensk Kärnbränslehantering AB
Swedish Nuclear Fuel
and Waste Management Co
Box 5864
SE-102 40 Stockholm Sweden
Tel 08-459 84 00
+46 8 459 84 00
Fax 08-661 57 19
+46 8 661 57 19

ISSN 1402-3091
SKB Rapport R-05-86

Bedrock transport properties

Preliminary site description Forsmark area – version 1.2

Johan Byegård, Eva Gustavsson, Geosigma AB

Eva-Lena Tullborg, Terralogica AB

Jan-Olof Selroos, Svensk Kärnbränslehantering AB

December 2006

Keywords: Retardation model, Transport properties, Forsmark, Fracture mineralogy, Diffusivity, Porosity, Sorption.

Abstract

A preliminary description on the retardation properties in the rock-groundwater environment in the Forsmark site investigation area has been made. The description is based on the available geological, hydrogeochemical and transport data (e.g. porosity, diffusivity and sorption properties). The outcome is summarized in tables which give the retardation properties for intact rock and for different types of fracture materials in the Forsmark site investigation area. This is a first outline of this retardation model which is aimed to be more sophisticated in forthcoming versions as more data will be available.

The major rock type present in the candidate area is a medium-grained, biotite-bearing granite to granodiorite, metamorphic. Besides that, a number of minor rock types are present among which a fine- to medium-grained granodiorite, tonalite and granite is the most commonly found.

Concerning the fractures and minor deformation zones; five different types of fracture coatings have been identified and described, together with three different sets of hydraulically active deformation zones.

For the hydrogeochemistry concerned, a description of the different water groundwater types at different dept are given. These groundwater types are compared to the different water types that were identified and used in the laboratory experiments (i.e. diffusion and batch sorption experiment).

Data are presented and are discussed for the results of the on-going investigations of porosity measurements, resistivity measurements (laboratory and in situ) as well as the through diffusion experiments. No results are at the present stage available for the batch sorption measurements. However, information from the active surface area measurements (BET surface area measurements) are presented which can be expected to provide information concerning some general sorption capacity of the different Forsmark rock types and/or fracture types. Both for the porosity and the diffusivity data, the results indicate that a log-normal distribution model is more appropriate compared to a normal distribution.

Comparisons between the resistivity measurements in situ and on sampled drill core measured in laboratory, indicate a sample disturbance which gives an overestimation of the diffusivity (and most likely also the porosity) on rock samples exposed to stress release. Some indications are obtained that these differences can be correlated to similar trends obtained for the P-wave measurements performed within the rock mechanic programme. Because to the suspected overestimation of diffusivity in stress released laboratory samples, it has been decided in this stage to preferentially use in situ measured resistivity data instead.

The results of the resistivity and through diffusion experiments are expressed as formation factors; i.e. telling how much slower a non-sorbing substance diffuses in a particular porous rock type compared to the diffusion rate in pure electrolyte. For the major rock type, Granite to granodiorite, metamorphic, medium-grained, a porosity of $10^{-0.68\pm0.15}$ % and a formation factor of $10^{-4.68\pm0.24}$ are obtained. Concerning the other rock types studied, the results of porosity and formation factors are roughly in the same order; however, the episyenitic samples of the Granite to granodiorite, metamorphic, medium-grained strongly deviates with a porosity of $10^{-1.05\pm0.36}$ % and a formation factor of $10^{-2.25}$.

The results of the BET surface measurements indicates low values for the larger (1–2 mm) size fractions measured; i.e. in the range of 0.01–0.04 m^2/g for the Granite to granodiorite, metamorphic, medium-grained. The episyentic and altered samples of these rock types show somewhat higher BET surface areas. Furthermore, very high values can be observed for rock material associated with hydraulically conductive fracture zones (e.g. < 10.3 m^2/g), indicating a high sorption capacity in the vicinity of fractures.

Sammanfattning

En preliminär beskrivning har upprättats rörande retardationsegenskaper adresserat till berg/grundvatten-miljön för platsundersökningsområdet i Forsmark. Beskrivningen baserar sig på tillgängliga data för geologi, hydrogeokemi samt tranportegenskaper (t ex porositet, diffusivitet och sorptionsegenskaper). Resultaten sammanfattas i tabeller upprättade i syfte att beskriva retardationsegenskaperna för bergarterna samt spricktyperna som förekommer i Forsmarksområdet. Den aktuella rapporten är en första version av en sådan retardationsmodell som är menat att bli uppdaterad i framtida versioner av platsbeskrivningarna då mer data kommer att vara tillgängliga.

Den främst förekommande bergarten inom kandidatområdet är en metamorfisk medelkornig biotitinnehållande granit till granodiorit. Förutom denna så förekommer även ett antal bergarter i lägre förekomster, bland dem främst en fin till medelkornig granodiorit, tonalit och granit.

Beträffande sprickor och deformationszoner så har fem olika sorters spricktyper samt tre typer av hydrauliskt aktiva deformationszoner identifierats och beskrivits.

Rörande hydrogeokemin har en sammanfattande beskrivning upprättats om grundvattentyper vid olika bergsdjup. Dessa grundvattentyper jämförs i rapporten med de grundvattentyper som identifierades och sen har använts i laboratorieundersökningar (genomdiffusion och btchsorpt0insexperiment).

Data från det pågående programmet med porositetsmätningar, resistivitetsmätningar (lab samt in situ) såväl som genomdiffusionsförsök presenteras och diskuteras i rapporten. I detta skede finns dock inga data från batchsorptionsmätningarna tillgängliga för presentation. Resultat från mätningar av den aktiva ytan hos bergmaterialen (BET-yta) presenteras dock, vilket anses ge en generell kunskap om de olika bergmaterialens samt sprickornas sorptionskapacitet. För både porositets och diffusivitetsdata kan observeras att en lognormal fördelning beskriver spridningen av data bättre än vad som är möjligt med en motsvarande normalfördelning.

Jämförelser mellan in situ resistivitetsmätningar gjorda in situ och motsvarande mätningar utförda på provtagna borrkärneprover i laboratoriemiljö antyder att laboratoriemätningarna ger en förhöjd diffusivitet som orsakas av tryckavlastningen. Vissa indikationer presenteras på att dessa provstörningar är konsistenta med de trender som upptäckts i P-våg mätningar på borrkärnor, vilket utförts platsundersökningens bergmekanikprogram. På grund av misstankar om överskattning av diffusiviteten i laboratorieprover har det beslutats att i detta skede huvudsakligen använda resistivtetsdata erhållna från in situ mätningarna.

Resultaten från resistivitetmätningarna och från genomdiffusionsförsöken uttrycks i rapporten i form av formationsfaktorn, dvs, hur mycket långsammare ett icke-sorberande spårämne diffunderar i bergmaterialet jämfört med diffusionshastigheten i ren elektrolytlösning. För den vanligaste förekommande bergarten, metamorfisk medelkornig biotitinnehållande granit till granodiorit, rapporteras en porositet på $10^{-0.68\pm0.15}$ % och en formationsfaktor på $10^{-4.68\pm0.24}$. För de övriga bergarterna som studerats, ligger den uppmätta porositeten och formationsfaktorn i samma storleksordning; undantaget en episyenitisk form av huvudbergarten som visar en porositet på $10^{1.05\pm0.36}$ % och en formationsfaktor på $10^{-2.25}$.

Resultaten av BET-yte mätningarna visar låga värden för den store storleksfraktionen av krossad metamorfisk medelkornig biotitinnehållande granit till granodiorit, i intervallet 0.01–0.04 m^2/g. Den episyenitiska och den omvandlade formen av denna bergart visar något högre värden. Dessutom erhålls mycket höga värden (< 10.3 m^2/g) för bergmaterial från hydrauliskt konduktiva sprickzoner, vilket antyder en hög sorptionskapacitet hos material i anslutning till sprickor.

Contents

1 Introduction

1.1 Background

The Swedish Nuclear Fuel and Waste Management Company (SKB) is conducting site investigations at two different locations, the Forsmark and Simpevarp areas, with the objective of siting a geological repository for spent nuclear fuel. The results from the investigations at the sites are used as a basic input to the site descriptive modelling.

A Site Descriptive Model (SDM) is an integrated description of the site and its regional setting, covering the current state of the geosphere and the biosphere as well as ongoing natural processes of importance for long-term safety. The SDM shall summarise the current state of knowledge of the site, and provide parameters and models to be used in further analyses within Safety Assessment, Repository Design and Environmental Impact Assessment. The present report is produced as a part of the version 1.2 modelling of the Simpevarp area.

The process of site descriptive modelling of transport properties is described by /Berglund and Selroos 2004/. Essentially, the description consists of three parts:

- Description of rock mass and fractures/fracture zones, including relevant processes and conditions affecting radionuclide transport; the description should express the understanding of the site and the evidence supporting the proposed model.
- Retardation model: Identification and description of "typical" rock materials and fractures/fracture zones, including parametrisation.
- Transport properties model: Parametrisation of the 3D geological model and assessment of understanding, confidence and uncertainty.

The methods used within the transport programme produce primary data on the retardation parameters, i.e. the porosity, θ_m, the effective diffusivity, D_e, and the linear equilibrium sorption coefficient, K_d. These retardation parameters are evaluated, interpreted and presented in the form of a retardation model; the strategy for laboratory measurements, data evaluation and development of retardation models is described by /Widestrand et al. 2003/. In the three-dimensional modelling, the retardation model is used to parameterise the various geological "elements" (rock mass, fractures and fracture zones) in the site-descriptive geological model.

1.2 Conceptual model with potential alternatives

1.2.1 Basic conceptual model

The conceptual model underlying the site descriptive transport modelling is based on a description of solute transport in discretely fractured rock. Specifically, the fractured medium is viewed as consisting of mobile zones, i.e. fractures and fracture zones where groundwater flow and advective transport take place, and immobile zones in rock mass, fractures and fracture zones where solutes can be retained, i.e. be removed, temporally or permanently, from the mobile water /Berglund and Selroos 2004/. In the safety assessment framework that provides the basis for identification of retention parameters in the site descriptive models, retention is assumed to be caused by diffusion and linear equilibrium sorption. These processes are reversible and are here referred to as retardation processes.

The conceptualisation outlined above implies that radionuclide transport takes place along flow paths consisting of connected "sub paths" in fractures and fracture zones of different sizes. In this model, advection is the dominant process for moving the radionuclides in the transport direction, whereas the main role of diffusion is to remove the solutes from the mobile zone and transport them within the immobile zones, cf Figure 1-1. It should be noted that this conceptual model, and the present methodology for site descriptive modelling in general, are based on experiences from the Äspö Hard Rock Laboratory (ÄHRL), primarily the TRUE project (Tracer Retention Understanding Experiments) /Winberg et al. 2000, Poteri et al. 2002/, which are not necessarily fully applicable to the transport conditions at the Forsmark site.

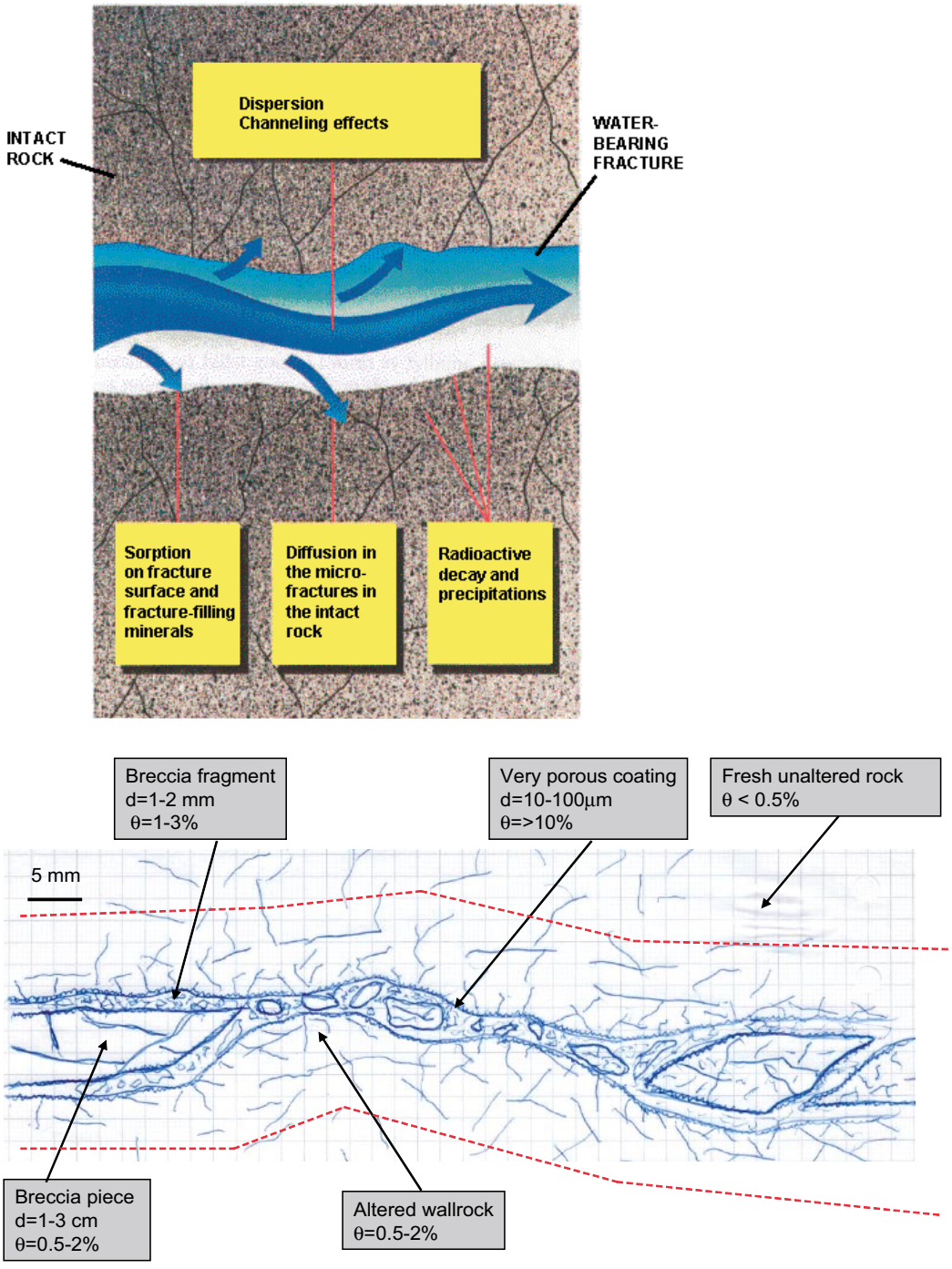

Figure 1-1. *Conceptualised drawing of transport processes (upper) given in comparison to a natural fracture (lower) based on observations in /Andersson et al. 2002/.*

1.2.2 Alternative processes and process models

Alternative conceptual models could involve alternative processes and/or alternative descriptions of the presently considered processes. Furthermore, different conceptualisations of the radionuclide transport paths, i.e. as advective flow paths in accordance with the basic conceptual model described above or with, for instance, diffusive transport in the mobile zone, could be considered. For radionuclide retention, consideration of alternative representations of sorption (process-based sorption models) and additional retention processes (e.g. precipitation and co-precipitation) are of particular interest.

Modelling activities involving process-based sorption models have been initiated during the F1.2 transport modelling. This modelling constitutes a first attempt on reactive-transport simulations in a single fracture, using data from ÄHRL /Dershowitz et al. 2003/. The aims are to gain experience on this type of modelling in a transport context, and to investigate whether the process-based sorption models show qualitative differences or specific features that cannot be reproduced with K_d-based models. Whereas such differences and features can be observed in the presently available results, it remains to be evaluated whether these effects may occur under realistic conditions. Hence, no conclusive results that could support, or provide alternatives to, the K_d-based model presented here are currently available.

1.3 Transport modelling in Forsmark 1.1

The Forsmark 1.1 (F1.1, for brevity) modelling of transport properties is described in /SKB 2004/. The main uncertainty identified in the 1.1 stage was related to the fact that no site investigation transport data were available. As further discussed below, this uncertainty will be only partly resolved in the Forsmark 1.2 (F1.2) model.

1.4 This report

The aim of the present report is to give a description of the development Forsmark 1.2 retardation model, and to give the background of the data that are used for the justification of the retardation model. Thus, the report focuses primarily on the first and second bullet points in the strategy outlined in Section 1.1. The data and models used as input to the modelling are described in Chapter 2, including the inputs from other modelling disciplines. Chapter 3 presents the evaluation of Transport data, whereas the resulting model is described in Chapter 4. Finally, Chapter 5 contains a brief discussion on the implications of the results for the continued investigations and modelling.

2 Description of input data

2.1 Data and models from other disciplines

2.1.1 Geology

The following summary and evaluation of geological data of relevance for the transport modelling is based on the F1.2 geological description, as presented in Chapter 5 of the F1.2 SDM report /SKB 2005a/, and the associated models and databases.

Rock groups and rock types

The Forsmark site area is dominated of intrusive, igneous rocks with subordinate supra-crustal rocks. Outcrop mapping on the mainland and in the archipelago area indicates four major groups of rock types − Groups A to D, Table 2-1. Mineralogical compositions of the different rock groups (and some of the rock types) are illustrated in Figure 2-1.

The major rock type in the candidate area is a medium-grained, biotite-bearing granite to granodiorite, metamorphic (rock code 101057) belonging to the Group B intrusive suite. This major rock type and subordinate rock types in the different rock groups are further described in Chapter 5 Forsmark SDM1.2 /SKB 2005a/.

Table 2-1. Major groups of rock types recognised during outcrop mapping at the Forsmark site. The geochronological data are discussed in Section 3.1. SKB rock codes are shown in brackets after each lithology. /Chapter 5 Forsmark SDM1.2, SKB 2005a/.

Rock types	
All rocks are affected by brittle deformation. The fractures generally cut the boundaries between the different rock types. The boundaries are predominantly not fractured.	
Rocks in Group D are affected only partly by ductile deformation and metamorphism.	
Group D (c 1,851 million years)	• Fine- to medium-grained granite and aplite (111058). Pegmatitic granite and pegmatite (101061). Variable age relationships with respect to Group C. Occur as dykes and minor bodies that are commonly discordant and, locally, strongly discordant to ductile deformation in older rocks.
Rocks in Group C are affected by penetrative ductile deformation under lower amphibolite-facies metamorphic conditions.	
Group C (c 1,864 million years)	• Fine- to medium-grained granodiorite, tonalite and subordinate granite (101051). Occur as lenses and dykes in Groups A and B. Intruded after some ductile deformation in the rocks belonging to Groups A and B with weakly discordant contacts to ductile deformation in these older rocks.
Rocks in Groups A and B are affected by penetrative ductile deformation under amphibolite-facies metamorphic conditions.	
Group B (c 1,886–1,865 million years)	• Biotite-bearing granite (to granodiorite) (101057) and aplitic granite (101058), both with amphibolite (102017) as dykes and irregular inclusions. • Tonalite to granodiorite (101054) with amphibolite (102017) enclaves. Granodiorite (101056). • Ultramafic rock (101004). Gabbro, diorite and quartz diorite (101033).
Group A (supracrustal rocks older than 1,885 million years)	• Sulphide mineralisation, possibly epigenetic (109010). • Volcanic rock (103076), calc-silicate rock (108019) and iron oxide mineralisation (109014). Subordinate sedimentary rocks (106001).

Figure 2-1. *Mineralogical composition of the analysed samples in the different rock groups (after /Stephens et al. 2005/).*

Rock domains

The focus is on rock domain RFM029 as it constitutes the major part of the local site. A few more rock domains are of interest as they constitute parts of KFM03 and KFM04:

RFM029 = dominantly granite to granodiorite, metamorphic (84%) subordinate pegmatite (2%), fine- to medium-grained granite (1%), fine- to medium-grained granodiorite, tonalite and granite (10%), amphibolite (3%).

RFM012 = dominantly granite to granodiorite, metamorphic (68%), subordinate fine- to medium-grained granodiorite, tonalite and granite (24%); pegmatite (4%), amphibolite (2%) and felsic to intermediate volcanic rock (2%).

RFM017 = dominantly tonalite to granodiorite, metamorphic, subordinate pegmatite and fine- to medium-grained granodiorite, tonalite and granite.

RFM018 = dominantly tonalite to granodiorite, metamorphic, subordinate granite to granodiorite, granodiorite, metamorphic, felsic to intermediate volcanic rock, amphibolite, fine- to medium- grained granodiorite, tonalite and granite.

2.1.2 Fractures and deformation zones

The conceptual fracture model consists of four sub-vertical sets and one sub-horizontal set, cf Section 5.5 in F 1.2 SDM. These sets are suggested based upon orientations, structural geometry and partly their fracture fillings. The steep fracture sets trend in N-S, NE-SW, NW-SE and E-W.

Fractures

Most of the fractures are initiated early in the geological history of the area and many show signs of later reactivation. There are no evidences of the sub horizontal fractures being younger than the vertical sets although they may have been reactivated during different time periods. In Table 2-2 the fracture intensities for the five sets are given related to the Rock Domains.

There is no consistent variation of fracture intensity with depth. However, the number of transmissive fractures intersected by the boreholes is much lower below 300 m depth. The four sub-vertical sets are probably part of much larger fracture sets that also include structural lineaments.

Most of the single fractures in the Forsmark area at depth larger than 100–150 m show low transmissivity, but still open and semi-open fractures are mapped through out the entire drillcores. It is therefore believed that the mineralogical composition of the fracture coatings are important as well as the presence or absence of an altered zone in the wall rock adjacent to the conductive fractures (Figure 2-2) as these fracture constitutes possible flow paths or more probable diffusion path ways. Table 2-3 show frequencies of fracture minerals in the open fractures for each core borehole based on Boremap data. It is important to keep in mind that this is based only on macroscopical observations of the drillcore which may influence the results mainly due to

1) difficulties in identification of some minerals without microscopy or analyses,

2) loss of loose and soft material during drilling.

It is therefore probable that the amounts of clay minerals are underestimated. Wall rock alteration is not so common around the open fractures (according to mapping less than 8%) but around the fractures that are water conducting (based on flow log) alteration seems to be much more common, although no exact figure is available. It is important to note and possibly also to further investigate that the number of mapped open fractures are very large (272–1,125) large compared to the fractures identified as water conducting by the flow log (a few tens or even fewer).

A more detailed evaluation of bore map data, hydraulic tests and the flow logging should provide important input to the transport modelling as it is believed that not all fracture types are equally transmissive.

Table 2-2. Intensity parameters as a function of rock domain, fracture type and fracture set from Section 5.5 in F1.2 SDM.

Rock domain ID	Fracture set	Intensity (P_{32} – m^2/m^3)			
		Open	Partly open	Sealed	Total
RFM029	NS	0.12	0.01	0.47	0.60
	NE	0.46	0.05	1.56	2.07
	NW	0.16	0.01	0.27	0.45
	EW	0.05	0.00	0.17	0.23
	HZ	0.34	0.01	0.26	0.61
	All	1.13	0.09	2.73	3.95
RFM018	NS	0.26	0.05	0.43	0.74
	NE	1.01	0.18	1.43	2.62
	NW	0.36	0.05	0.25	0.66
	EW	0.11	0.02	0.15	0.29
	HZ	0.73	0.04	0.24	1.01
	All	2.47	0.34	2.50	5.31
RFM017	NS	0.01	0.01	0.51	0.53
	NE	0.02	0.04	1.70	1.77
	NW	0.01	0.01	0.30	0.32
	EW	0.00	0.00	0.18	0.19
	HZ	0.02	0.01	0.28	0.31
	All	0.06	0.08	2.98	3.12
RFM012	NS	0.22	0.10	1.04	1.36
	NE	0.84	0.37	3.46	4.67
	NW	0.30	0.11	0.60	1.01
	EW	0.09	0.04	0.37	0.51
	HZ	0.61	0.09	0.57	1.27
	All	2.06	0.71	6.05	8.82

Table 2-3. Frequency of fracture coatings related to total number of open fractures.

Borehole	KFM01A	KFM02A	KFM03A	KFM04A	KFM05A	KFM06A
Chlorite and Epidote %	70	74.5	87.1	73.5	65.1	78.4
Quartz and Adularia %	1.1	3.2	1.1	4.1	1.7	9.2
Gouge %	0	0	0.4	0.2	0	0
Clay %	2.0	18.4	14.1	14.1	2	16.4
Laumontite %	18.6	0.4	0.7	7.3	10	6.6
Altered Wallrock %	0.3	6.2	3.3	2.8	7.7	4.1
Total number of open fractures	711	305	272	1,125	591	731

Description of fracture types

A. Chlorite ± calcite ± minor amounts of hematite

Mineralogy: chlorite, ± calcite ± hematite ± corrensite.

Usually thin coating, 0.5 mm on each side.

B. Chlorite and clay

Mineralogy: corrensite, illite, chlorite, ± epidote

1 mm thick coating on each side and > 3 cm wall rock alteration.

Common in water bearing fractures.

C. Chlorite and epidote or prehnite

Mineralogy: chlorite, ± prehnite or epidote or adularia ± calcite.

Usually 1–3 mm coating on each side with wall rock alteration around 1 cm.

D. Quartz

Mineralogy: quartz, calcite, pyrite, adularia.

Thin coating sometimes with larger (1–2 mm) solitary crystals of calcite or pyrite.

No wall rock alteration.

E. Laumontite

Mineralogy: laumontite, calcite ± chlorite/corrensite

Usually 1 mm with wall rock alteration ca 1 cm on each side

Deformation zones

Concerning deformation zones four sets have been identified /SKB 2005a/; these are:

- Vertical and steeply, SW-dipping deformation zones that strike WNW-NW, and are dominated by sealed fractures. These zones initiated their development in the ductile regime but continued to be active in the brittle regime. On the basis of their length, both regional and local major zones are present. The model also includes one local minor zone, which has been identified with high confidence, as well as subordinate zone segments that are situated close to and are attached to regional and local major zones. These segments are both local minor and local major in character.
- Vertical and steeply dipping deformation zones that strike NE and are also dominated by sealed fractures. These zones formed in the brittle regime and length estimates indicate that no zones are longer than 10 km. Two local minor zones, which have been recognised with high confidence, have also been modelled. Furthermore, the model includes two subordinate zone segments that are local minor in character, and are situated close to and are attached to two local major zones. A zone that does not extend to the surface has also been included.
- Vertical and steeply dipping deformation zones that strike NS and are also dominated by sealed fractures. These zones formed in the brittle regime and length estimates indicate that no zones are longer than 10 km. With the exception of one local minor zone, which has been identified with medium confidence, all zones have been recognised with low confidence. Relative to the other three sets, this set is of subordinate significance in the regional model volume.
- Gently SE- and S-dipping deformation zones that formed in the brittle regime and that, relative to the other sets, contain a higher frequency of open fractures. Length estimates indicate that no zones are longer than 10 km. However, due to truncation or their gentle dip, several of these zones fail to reach the surface inside the regional model volume.

For the retardation model, the hydraulically conductive parts of the zones are of greatest interest since not all geologically identified deformation zones are found to be hydraulically conductive. In addition, there is a significant heterogeneity observed among the conductive zones. Based on the interpretations from the boreholes, three different sets of conductive deformation zones have been possible to identify (and partly also to sample). These are:

1. The NW trending zones, characterised by ductile deformation (presence of mylonites) and altered wall rock as well as later brittle deformation. The water conducting fractures are coated with chlorite and clay minerals ± calcite ± epidote. This type of zone is intersected in boreholes HFM11 and HFM12 (Eckarfjärden deformation zone). However, it also includes the Singö deformation zone that was studied in older investigations at Forsmark.
2. The NE trending steep brittle deformation zones characterised by laumontite sealed brecciated wall rock with a few open fractures coated with laumontite ± chlorite and calcite. This zone type is present e.g. in KFM05A. Results from the hydro tests indicate that this zone type has lower transmissivity than zone type 1 and 3. However increasing transmissivity closer to the surface may be expected.
3. The SE gently dipping brittle deformation zones characterised by a higher frequency of open fractures. The open water conducting fractures are coated with chlorite and clay minerals ± quartz ± adularia ± calcite. The wall rock is altered and often cataclastic. These are the zones with high transmissivities regardless of depth. This type of zone is e.g. present in KFM02A and KFM03A.

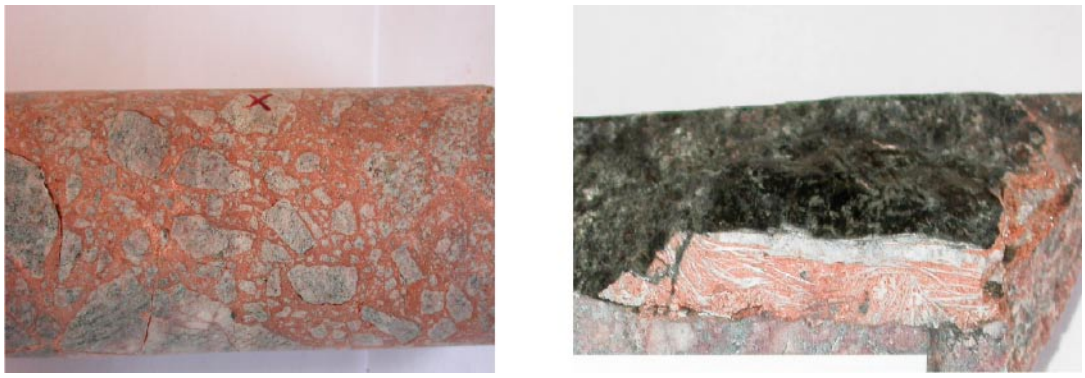

Figure 2-2. *Examples of deformation zone, type 2. To the left: laumontite sealed breccia, to the right; open fracture in the deformation zone with laumontite, calcite, chlorite.*

Figure 2-3. *Examples of altered rock coated with chlorite and clay minerals in transmissive part of SE gently dipping brittle deformation zones.*

In addition, a superficial interval of sub-horizontal "fractures" is encountered in several boreholes in the upper 100/150 m, predominantly in the north-western part of the candidate area. These features are sometimes found to be fully open and highly transmissive. They are sometimes completely filled with gouge-like material or, if they are very close to the surface, fine-grained sediments, in which cases they are of very low transmissivity. The explanation of these shallow sub-horizontal "fractures" and their possible relation to the set of deformation zones in group 3 is not fully resolved at present. The gouge-like material in the shallow structures contains quartz, adularia, chlorite and mixed layer clays. The wall rock is altered.

Detailed information from the zones such as flow patterns within the zone (e.g. channelling etc) and internal structure; for example amounts of soft and fine grained material and its structure in situ, is not available for this model version.

2.1.3 Hydrogeochemistry

The hydrogeochemical modelling of the Forsmark area is based on data from the core boreholes KFM01A–KFM04A and from the percussion boreholes HFM01–HFM19. The results are presented in Chapter 9 of the F1.2 SDM report /SKB 2005a/. The overall understanding of the groundwater system at Forsmark is summarised in the figure below.

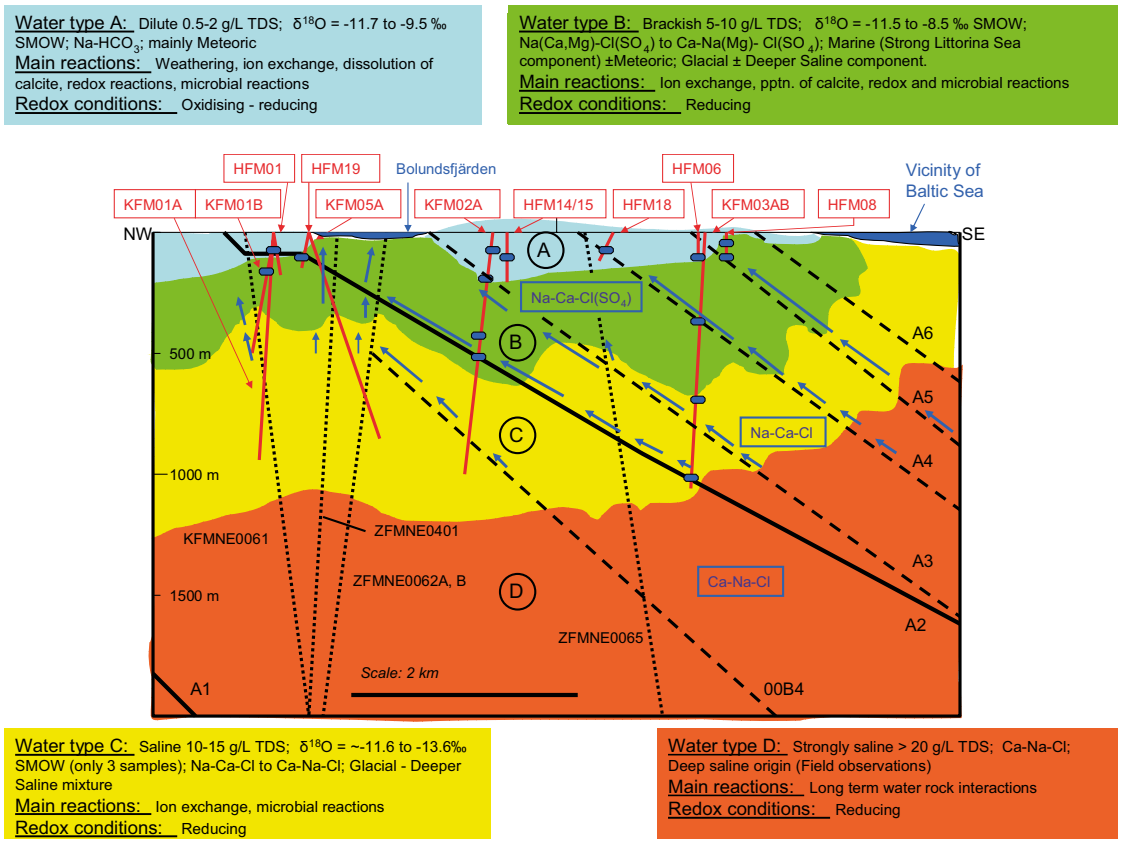

Figure 2-4. *Schematic 2-D model based on integrating the major structures, the major groundwater flow directions and the different groundwater chemistries. The blue arrows are estimated groundwater flow directions and their respective lengths reflect relative groundwater flow velocities (short = low flow; longer = larger flow) /SKB 2005b/.*

Water of salinity close to the one measured at repository depth has been used for the diffusivity measurements. A water composition (described as type II) was chosen; however, only the major components (i.e. Ca^{2+}, Na^{+}, Cl^{-} and SO_4^{2-}) were included for the diffusion experiments.

For the batch sorption experiments, the groundwater composition is considered to be more important, and four different groundwater compositions have therefore been selected, as follows:

I. Fresh diluted Ca-HCO3 water; groundwater now present in the upper 100 m of the bedrock, but also a water type that can be found at larger depths during late phases of glacial periods.

II. Groundwater with marine character, Na-(Ca)- Mg-Cl (5,000 mg/L Cl); This is constitute a large portion of the groundwaters found at 150 to 600 m depth at Forsmark. It is assumed to originate from the Littorina stage of the postglacial Baltic Sea

III. Saline groundwater of Na-Ca-Cl type (5,400 mg/L Cl); this is a water with higher Ca and lower Mg compared to the type II water.

IV. Brine type water of very high salinity, Ca-Na-Cl type water with Cl content of 45,000 mg/L; during a glacial period, brine type waters can be forced to more shallow levels than at present.

The compositions of these groundwater types are specified in Table 2-3 below, referring to specific sampling intervals in the boreholes.

Table 2-3. Water classification of the Forsmark area; concentrations are given in mg/L.

	Type I (HSH02 0–200 m) Fresh water	Type II (KFM02A 509–516 m) Groundwater with marine character (present groundwater at repository level)	Type III (KFM03 639–646 m) Saline groundwater	Type IV (KLX02 1,383–1,392 m) Brine type water of very high salinity
Li^+	1.60E–02	5.10E–02	2.80E–02	4.85E+00
Na^+	1.27E+02	2.12E+03	1.69E+03	7.45E+03
K^+	2.16E+00	3.33E+01	1.42E+01	3.26E+01
Rb^+	(2.52E–02)[A]	6.28E–02	3.93E–02	1.78E–01
Cs^+	(1.17E–03)[A]	1.79E–03	7.09E–04	1.86E–02
NH_4^+	(9.47E–02)[A]	4.00E–02	2.04E–01	5.60E–01
Mg^{2+}	1.43E+00	2.32E+02	5.27E+01	1.20E+00
Ca^{2+}	5.21E+00	9.34E+02	1.47E+03	1.48E+04
Sr^{2+}	6.95E–02	7.95E+00	1.69E+01	2.53E+02
Ba^{2+}	(1.29E+00)[A]	1.88E–01	9.07E–02	2.40E–02
Fe^{2+}	(3.64E–01)[C]	1.20E+00	2.33E–01	3.45E+00
Mn^{2+}	2.00E–02	2.12E+00	3.18E–01	1.11E+00
F^-	3.03E+00	9.00E–01	2.04E–01	(1.60E+00)[D]
Cl^-	2.15E+01	5.15E+03	5.19E+03	3.68E+04
Br^-	(2.00E–01)[B]	2.20E+01	3.89E+01	5.09E+02
SO_4^{2-}	8.56E+00	5.10E+02	1.95E+02	1.21E+03
Si(tot)	6.56E+00	5.20E+00	6.28E+00	2.60E+00
HCO_3^-	2.52E+02	1.24E+02	2.19E+01	4.20E+01
S^{2-}	(1.00E–02)[B]	5.00E–02	2.95E–02	5.00E–02
pH	8.58	7.1	7.55	6.8

[A)] No measurements available, data imported from KSH01 #5263.
[B)] Based on detection limit.
[C)] Based on the Fe-tot measurement.
[D)] No measurements available, data imported from KLX02 #2731.

2.2 Transport data

2.2.1 Site investigation data

Laboratory investigations within the Transport programme are proposed to give site-specific sorption and diffusion properties for different rock types and fracture types. Rock samples for the laboratory measurements have been selected from KFM01A, KFM02A, KFM03A, KFM04A, KFM05A and KFM06A, in accordance with /Widestrand et al. 2003/. In order to describe the heterogeneity of the retardation parameters and the possible effects of stress release, rock samples are selected from different depths in the boreholes. The selection of samples from fractures/fracture zones were mainly controlled by the indications of water flow, as recorded in flow logs. The selection of samples from fractures/fracture zones was mainly controlled by the indications of water flow, as recorded in flow logs.

The sample collection consists of about 320 rock samples, mainly from the major rock type, fractures and deformation zones. However, it also includes samples of altered bedrock and minor rock types. Data available for the F1.2 modelling are however rather limited since diffusion and sorption measurements are in progress at Chalmers University of Technology

(CTH) and at the Royal Institute of Technology (KTH). Data from water saturation porosity measurements on different rock types and specific surface area data (BET, /Brunauer et al. 1938/), mainly from major and minor rock types are included in this report. PMMA porosity measurements and He-gas through-diffusion measurements are planned to be performed during spring 2005.

Table 2-4. Rock sample data included in the retardation model.

Number of rock samples	Non available rock sample data (diff, batch, resistivity, PMMA)	BET	Available rock sample data porosity	resistivity	Rock samples not yet included
317	158	22	172	79	80

3 Analyses and evaluation of transport data

In this chapter, the data used (site-specific and/or imported from other works) for establishing the retardation models are described. According to the basic conceptual model for radionuclide retention, Section 1.2.1, the considered retardation processes can be described as:

A. Adsorption on surfaces of materials present in or at the fracture walls, which are considered to be directly accessible (no significant diffusion needed) during the transport. These fracture surface reactions are considered to be independent of the flow rate and the residence time in the fracture, and can thus be simply described by an equilibrium surface sorption coefficient, K_a (m). The retardation obtained by this process can be described by a retardation factor, R_f, defined as:

$$R_f = 1 + \frac{2K_a}{b},$$

where b is the aperture of the fracture.

B. Diffusion into the rock matrix and a potential adsorption on the inner surfaces of the rock material. This process is dependent on the following parameters:

   a. The amount of inner volume (pores) in the rock matrix that is available for diffusion, i.e. the porosity, θ_m (–).

   b. The rate at which the radionuclide diffuses in the rock matrix, i.e. the effective diffusivity, D_e (m^2/s).

   c. The partitioning coefficient describing the distribution of the radionuclide between the inner surfaces of the pores and the water volume of the pores, K_d (m^3/kg).

In the time perspective relevant for storage of nuclear waste, the A process can often be neglected compared to the B process.

3.1 Porosity

3.1.1 Methods

Porosity refers to the volume of the rock that is filled with water and available for diffusion. With the concept used in this work, the porosity is considered in the micro scale to be homogeneously distributed in the rock matrix. Studies of the spatial distribution of porosity in the micro scale (PMMA, SKB MD 540.003) are planned in the site investigation programme, but have not been performed so far.

The porosity data used in the site descriptive transport modelling has mainly been obtained from measurements done on rock samples aimed for diffusion and sorption studies. The method used for determination (SS-EN 1936) consists of a water saturation of the sample, followed by a drying step. The drying of the samples is done at a temperature of 70° C, which differs from the temperature (105°C) used in the method for porosity measurements in the geology programme of the site investigation (SKB MD 160.002). The reason for this is that the samples in the transport programme are designated for other laboratory investigations afterwards. For the interpretation of these laboratory investigations (diffusion and sorption measurements), it is important to avoid the extra chemical and mechanical degradation of the samples that could result from the higher drying temperature.

It should also be emphasized that a measurement of the porosity is also obtained in the through-diffusion measurements (cf Section 3.2). From the fitting of the experimental results to the diffusion model, the capacity factor (α) is obtained, which for the non-sorbing tracer HTO should be equivalent to the porosity. However, the main source of porosity data in this work will be the water saturation measurements. Capacity factor measurements will only be used for comparisons.

The results of the porosity measurements are summarized in Table 3-1, and are also presented on a detailed sample level in Appendix 1. The geological characterisation in binocular microscope shows a great number of small cracks that are 3–15 mm in length and with a width of ≤0.5 mm, in both fresh and altered rock samples. These cracks are thus larger than intragranular micro cracks /Ståhle 2001/, and cut right through mineral grains. In Table 3-1, it is indicated that these cracks may increase the porosity.

There are also other factors that may affect the porosity; one factor is the alteration of rock, another is the length of the rock sample. For this reason, samples with observed alteration were studied separately and an indication of increased porosity for these samples can be observed. In this stage of the laboratory investigations, there is not very much data to clearly support the theory of alteration effects, but it has also been shown in previous investigations /Eliasson 1993/ and should be considered in forthcoming evaluations of data from the on-going site investigations.

The strongly altered episyenetic samples show a very significant increase in porosity compared to all other rock types included in this study.

The effect of the sample length is illustrated in Table 3-2, which indicates that the measurement method gives an increase in measured porosity values with shorter sample lengths. The effect of increased porosity value is, however, almost only observed for the 0.5 cm samples. Contrary, for the very porous (10–20%) episyenetic rock, it is indicated that the measurements give a lower porosity for the 0.5 cm samples and possibly also for the 1 cm samples. The reason for this is not fully understood but a possible explanation could be that such thin samples cause the water to easily escape out of the pores when taking them out of the water bath.

The statement of increased porosity with shorter sample length is supported by earlier porosity measurements in connection with diffusion experiments /Johansson et al. 1997/.

Table 3-1. Porosities (vol-%) of different rock types from the Forsmark area (number of samples within parenthesis). Mean value ± one standard deviation of experimental data set; in italics mean value, standard deviation of log_{10} of experimental data set (log_{10} of the data).

Rock type (SKB code)	All rock samples (n)	Rock samples without visible cracks (n)
Granite, granodiorite and tonalite, metamorphic, fine- to medium-grained (101051)	0.30 ± 0.27 (30) *–0.60,0.23* only altered samples: 0.50±0.51 (7)	0.25 ± 0.11 (28) *–0.64,0.17* only altered samples: 0.30±0.18 (5)
Granite to granodiorite, metamorphic, medium-grained, episyentic samples excluded. (101057)	0.24 ± 0.12 (105) *–0.66,0.17* only altered samples: 0.31±0.20 (18)	0.22 ± 0.09 (95) *–0.68,0.15* only altered samples: 0.26±0.20 (12)
Granite to granodiorite, metamorphic, medium-grained, episyenite (101057)	14 ± 6 (15) *1.05,0.36*	No samples excluded

Rock type (SKB code)	All rock samples (n)	Rock samples without visible cracks (n)
Pegmatite, pegmatitic granite (101061)	0.42 ± 0.23 (3) *–0.41,0.22*	No samples excluded
Amphibolite (102017)	1.8 ± 4.0 (6) *–0.46,0.76*	0.21 ± 0.12 (5) *–0.75,0.28*
Granodiorite, metamorphic (101056)	0.34 ± 0.21 (2) *–0.52,0.28*	No samples excluded
Felsic to intermediate volcanic rock, metamorphic (103076)	0.78 (1) *–0.11*	No samples excluded

Table 3-2. Porosities (vol-%) for rock samples of different lengths (number of samples within parenthesis). Mean value ± one standard deviation of experimental data set.

	Samples 0.5 cm (n)	Samples 1 cm (n)	Samples 3 cm (n)	Samples 5 cm (n)
Granite, granodiorite and tonalite, metamorphic, fine- to medium-grained, KFM02A, 541 m	0.34 ± 0.17 (3)	0.20 ± 0.12 (3)	0.19 ± 0.08 (3)	0.18 ± 0.10 (3)
Granite to granodiorite, metamorphic, medium-grained, KFM01A, 313 m	0.26 ± 0.11 (3)	0.18 ± 0.03 (3)	0.12 ± 0.08 (3)	0.16 ± 0.03 (3)
Granite to granodiorite, metamorphic, medium-grained, KFM01A, 276 m (episyenetic samples)	10.5 ± 1.1(3)	16.5 ± 0.3 (3)	18.3 ± 1.1 (3)	18.5 ± 0.6 (3)

3.2 Diffusion

3.2.1 Methods and parameters

In this work, the term diffusion refers to the process in which a tracer can diffuse from the fracture water volume into the micro fractures of the rock matrix. Thereby, an interaction can occur in which the inner surfaces of the rock matrix can be available for sorption, and the tracers can be significantly retarded in their transport. This work addresses diffusion processes in the aqueous phase only; potential diffusive mobility in the adsorbed state (so-called surface diffusion /Ohlsson and Neretnieks 1997/) has not been considered.

In this work, primarily two methods are used for the determination of the diffusivity of the rock materials /Widestrand et al. 2003/:

- Through-diffusion measurements; a method where the effective diffusivity, D_e (m^2/s), is determined by studying the diffusion rate of tritiated water (HTO) through a rock sample (HTO is used in the site investigations; the method can be applied also with other tracer solutions).
- Resistivity measurements; a method where the information on the diffusivity is obtained from the resistivity of electrolyte-saturated rock samples.

The diffusion process is quantified in terms of the formation factor, F_m (–). This parameter quantifies the reduced diffusion rate obtained in the rock material relative to the diffusion rate in pure electrolyte. It is thus calculated from the results of the through-diffusion studies, as:

$$F_m = \frac{D_e}{D_w} \tag{3-1}$$

where D_w (m^2/s) is the diffusivity of tritiated water in pure water, i.e. 2.13E–9 m^2/s /Li and Gregory 1974/.

For the resistivity measurements, F is the parameter produced by the method, i.e. the ratio of the resistivity of a given electrolyte to the resistivity of the rock sample with the pores saturated with the same electrolyte.

The resistivity can be measured both in laboratory experiments (where the rock samples are saturated with 1 M NaCl) and in borehole in situ experiments. For obvious reasons, no saturation of the rock matrix with a known electrolyte can be done in in situ experiments. In this case, the composition of the pore liquid must be estimated based on hydrogeochemical sampling and analysis, commonly assuming the same composition in the matrix as in the groundwater in neighbouring fractures. A further complication is that a lower salinity than 1 M NaCl, which thus likely could be present in the pores in in situ rock, according to /Ohlsson and Neretnieks 1997/ attributes a significant part of the conductivity to the surface ion mobility.

3.2.2 Through-diffusion studies

Site-specific data

Site specific rock materials from the Forsmark site have been sampled and used in through-diffusion measurements according to SKB MD 540.001 (SKB internal document). These measurements are time consuming, and steady state conditions (necessary for final evaluation) have not been obtained in most samples. However, for the parameterisation of the F1.2 retardation model, a selection of results from on-going through diffusion experiments has been done. Based on these data, preliminary diffusivities were evaluated.

The determination of diffusivity according to SKB MD540.001 (SKB internal document) is performed by studying the diffusion of tritiated water (HTO) through a slice of rock. A slice of water-saturated rock is mounted in a diffusion cell, where the start cell is filled with water spiked with HTO tracer and the other side is filled with non-spiked water. The diffusion is determined from the rate of the in-growth of the HTO tracer in the originally non-spiked water volume. The effective diffusivity, D_e (m^2/s) and the rock capacity factor, α (–) is calculated by fitting the model equation:

$$C_r = \frac{C_2 V_2}{C_1 A l} = \frac{D_e t}{l^2} - \frac{\alpha}{6} - \frac{2\alpha}{\pi^2} \sum_{n=1}^{\infty} \frac{(-1)^n}{n^2} \exp\left\{ - \frac{D_e n^2 \pi^2 t}{l^2 \alpha} \right\} \tag{3-2}$$

where C_2 (Bq/m^3) is the accumulated tracer concentration in the target cell at the time t (s), V_2 (m^3) is the volume of the target cell, C_1 (Bq/m^3) is the tracer concentration in the start cell, A (m^2) is the geometric surface area of the rock sample, and l (m) is the length of the rock sample. The results of the preliminary evaluation of the on-going through diffusion experiments are presented in Table 3-3. In this table, comparisons of the results to corresponding electrical resistivity measurements (Laboratory and in situ) are also presented.

From the results, it can be concluded that formation factors in the interval of 1.0E–4 to 1.5E–4 is observed both for the Granite, granodiorite and tonalite, metamorphic, fine- to medium-grained sampled at 555 m in KFM02A and for the Granite to granodiorite, metamorphic, medium-grained sampled at 313 m in KFM01A. One measurement is also available for the latter rock type from a depth of that shows a through diffusion determined formation factor of 4.3E–4 (5.1E–4) for the corresponding electrical resistivity measurement). Altogether, these observations indicate a fairly good agreement between these two methods.

The Granite to granodiorite, metamorphic, medium-grained sample from 281.00 m has a formation factor that is significantly higher than all other measured formation factor. This is not surprising since this is a sample with episyenetic alteration, i.e. having a porosity of ~10%.

Any dependence of the measured diffusivity increasing with decreasing sample length is difficult to observe with the relatively low number of sample used (cf Figures 3-1).

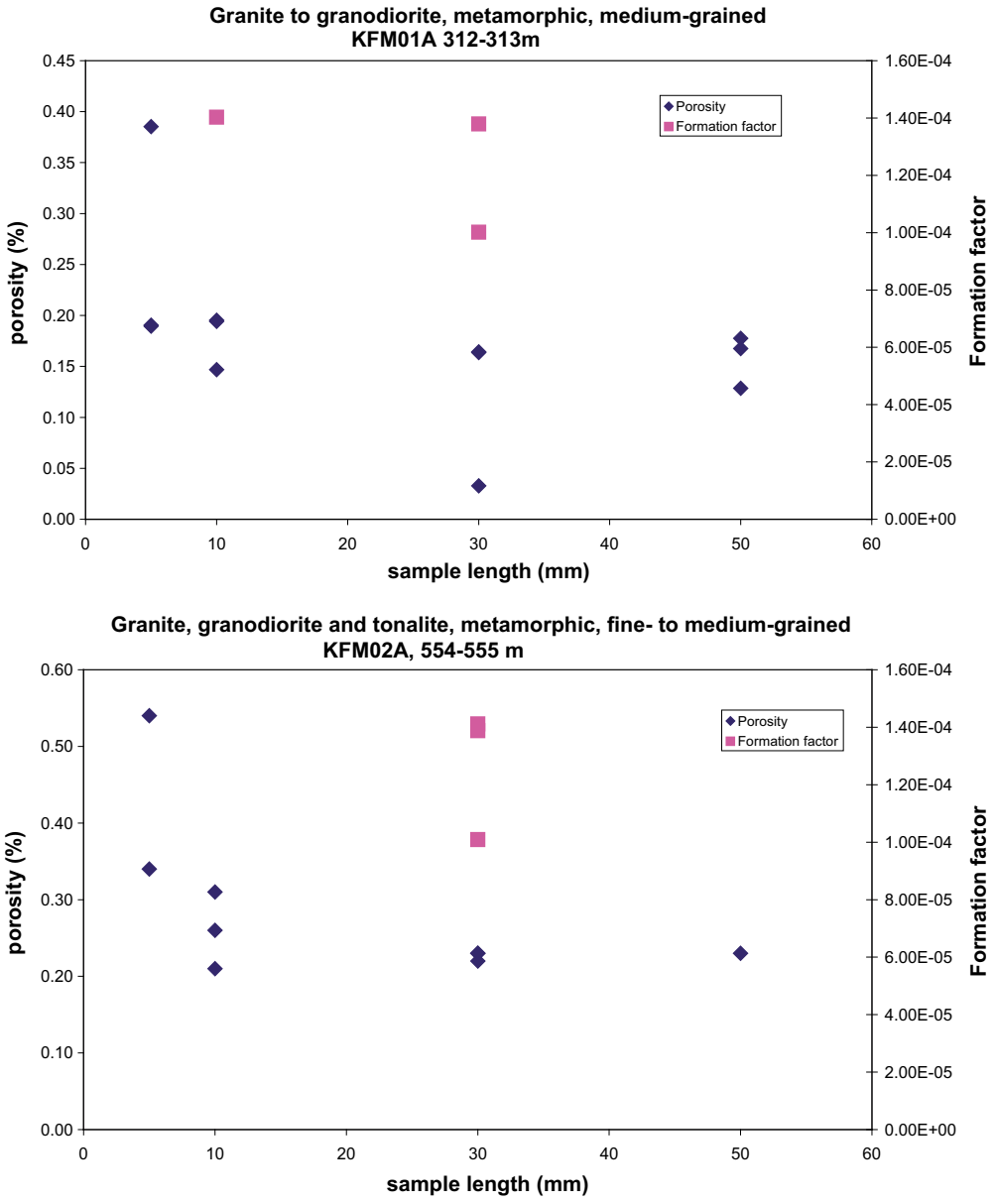

Figure 3-1. *Measured porosity and formation factor (obtained by through diffusion experiment) as a function of the length of the sample used in the measurements.*

Table 3-3. Preliminary results from through-diffusion experiments on rock samples from KFM01A and KFM02. The effective diffusivity, D_e, and the rock capacity factor, α, were obtained from least-square fits to experimental data. Formation factors were calculated from Equation (3-1). Comparisons are made to the porosity obtained by water saturation measurements and to the formation factors obtained from closest available electrical resistivity measurements (Lab and in situ).

Rock type (SKB code)	SKB ID	Sample thickness (mm)	α (–)	θ (water saturation)	D_e (m^2/s)	F_m (through-diffusion)	F_m (resistivity lab, closest available measurement)	F_m (resistivity in situ, closest available measurement)
Granite, granodiorite and tonalite, metamorphic, fine- to medium-grained (101051)	KFM02A 554.61–554.64 m	30	3.39E–03	2.3E–03	2.15E–13	1.01E–04	1.52E–04	pending
	KFM02A 554.72–554.7 5 m	30	4.56E–03	2.2E–03	2.96E–13	1.39E–04	1.52E–04	pending
	KFM02A 554.86–554.89 m	30	5.31E–03	2.3E–03	3.01E–13	1.41E–04	1.52E–04	pending
Granite to granodiorite, metamorphic, medium-grained (101057)	KFM01A 312.56–312.59	30	2.92E–03	1.6E–03	2.13E–13	1.00E–04	1.52E–04	9.58E–06
	KFM01A 312.66–312.67	10	1.69E–02	1.9E–03	2.99E–13	1.40E–04	1.52E–04	9.58E–06
	KFM01A 312.68–312.71	30	4.38E–03	1.6E–03	2.94E–13	1.38E–04	1.52E–04	9.58E–06
	KFM01A 312.77–312.78	10	1.91E–02	1.5E–03	3.19E–13	1.50E–04	1.52E–04	9.58E–06
	KFM01A 999.95–1,000.00	30	8.65E–03	2.4E–03	9.12E–13	4.28E–04	5.11E–04	1.09E–05
	KFM02A 281.00–281.05 (episyenetic)	30	5.81E–02	1.105E–1	1.25E–11	5.86E–03	pending	pending

3.2.3 Electrical resistivity

A summary of the results of the electrical resistivity measurements reported by /Löfgren and Neretnieks 2005, Thunehed 2005/ is provided in Table 3-4; the individual measurement results can be found in Appendix 2. Some general observations made from these results are presented in the following.

Laboratory resistivity measurement compared to through diffusion measurements

The comparison between laboratory resistivity measurements and through diffusion measurements on samples from similar location indicate a very good correlation between these measurements; possibly with a tendency of the formation factor from the through diffusion experiments somewhat lower then the corresponding values from the electrical resistivity measurements. When comparing the results from all formation factor measurements (Figure 3-2), it is, however, indicated that the results from the through diffusion measurements are found in the lower part of the diagram. This could be an indication that through-diffusion measurements gives lower formation factors than electrical resistivity measurements, as was indicated in /Widestrand et al. 2003/. However, the number of through diffusion measurements is from the basis of this report too low to conclude any clear difference of the results of the two methods.

Laboratory resistivity versus porosity

As expected, a tendency of increased formation factor with increasing porosity can be observed in the results (Figure 3-2). However, it is obvious that the data cannot be described by a normal distribution, neither for the formation factor nor for the porosity. A presentation

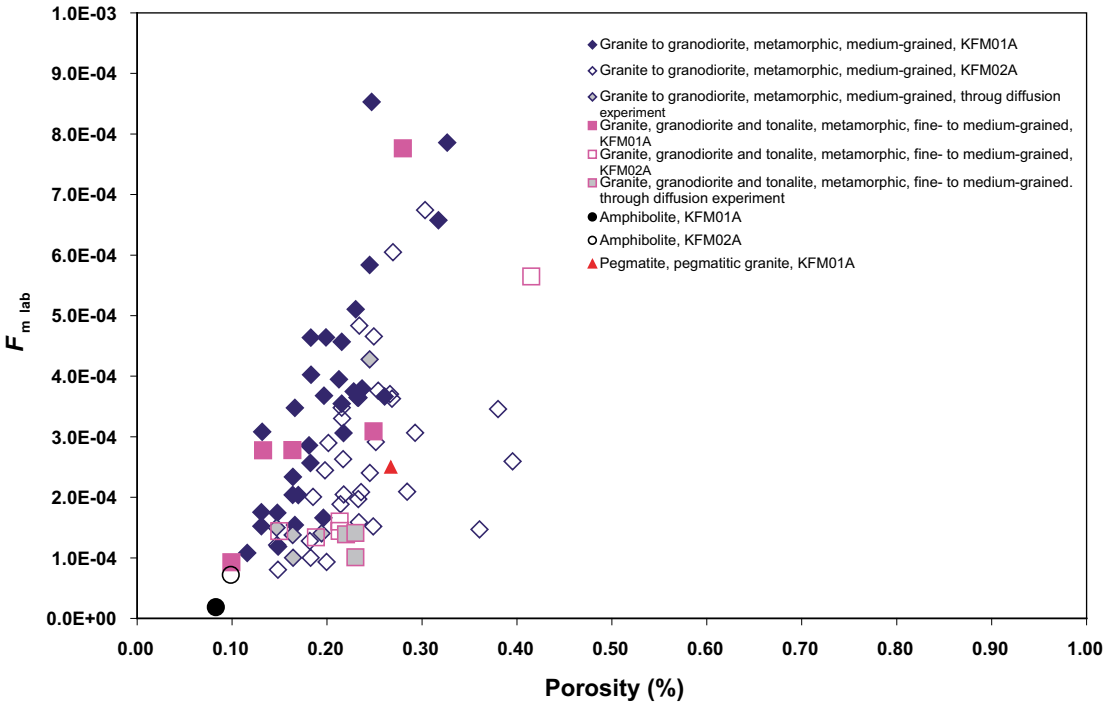

Figure 3-2. *Formation factor versus the porosity, formation factor determined from electrical resistivity measurements in the laboratory /Löfgren and Neretnieks 2005/. Comparisons are made to formation factors determined by through diffusion experiments, The porosities have been measured using the water saturation method (SS-EN 1936).*

of the data in log-log scale (Figure 3-3) indicates that the porosity and diffusivity characteristics should instead be described using log-normal distributions. Distribution plots for formation factors and porosity data for samples consisting of Granite to granodiorite, metamorphic, medium-grained (Figures 3-4 and 3-5) indicates a reasonably log-normal distribution of the porosity, whereas the formation factor does not show as good log-normal distribution as the porosity.

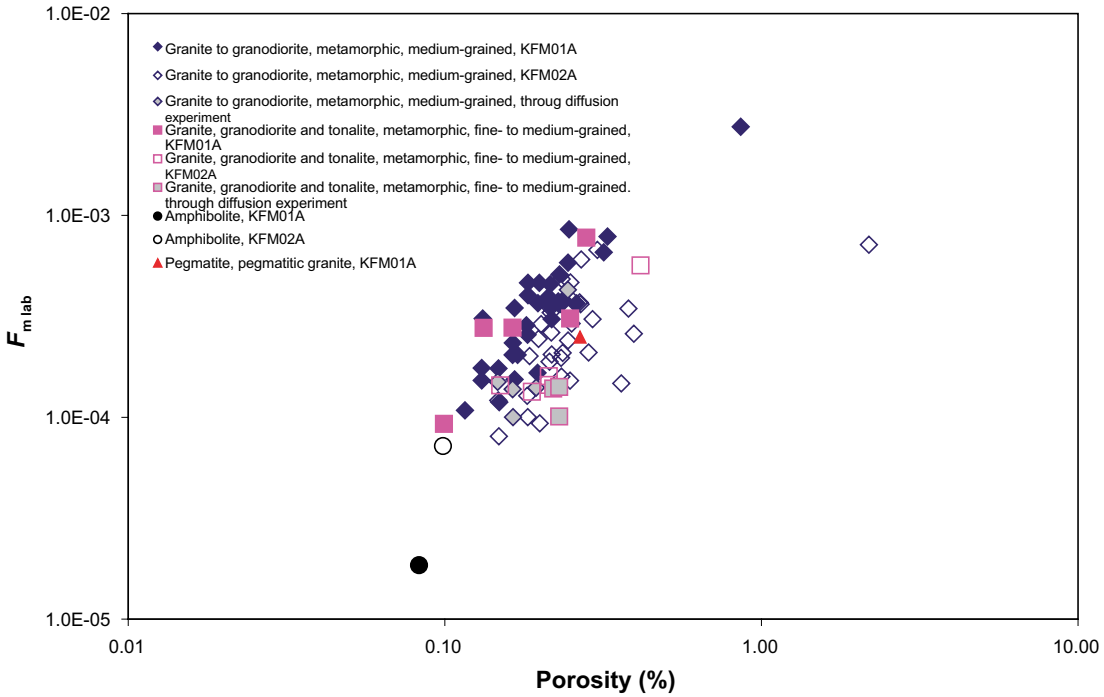

Figure 3-3. *Formation factor versus the porosity (in log-log scale), formation factor determined from electrical resistivity measurements in the laboratory /Löfgren and Neretnieks 2005/. The porosities have been measured using the water saturation method (SS-EN 1936).*

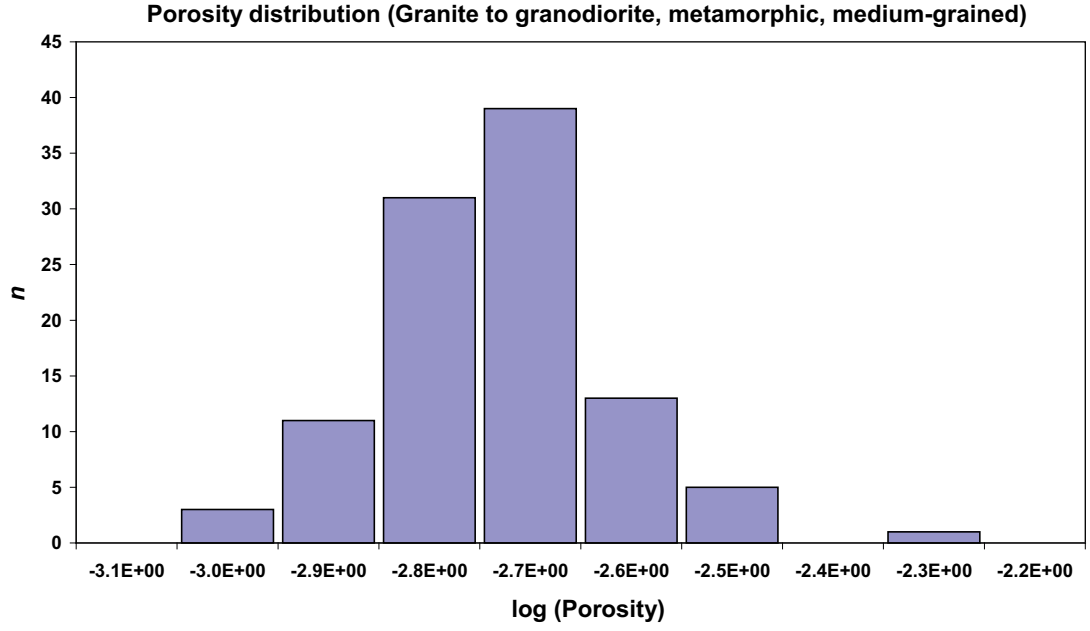

Figure 3-4. *Distribution of porosity in the log-scale for the Granite to granodiorite, metamorphic, medium-grained, samples.*

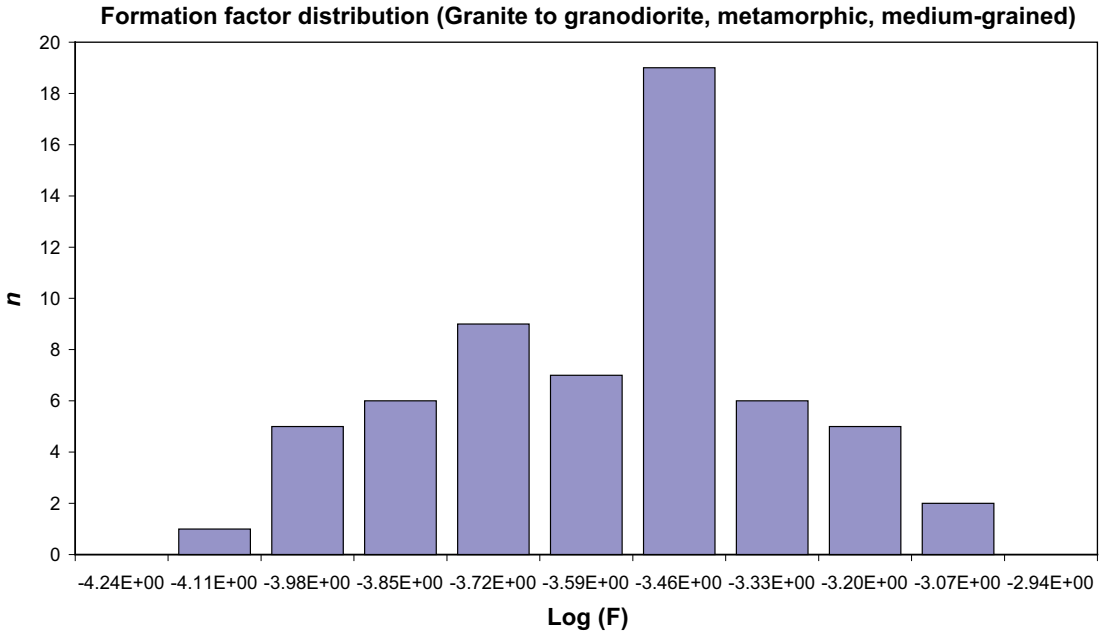

Figure 3-5. *Distribution of the formation factor in the log-scale for the Granite to granodiorite, metamorphic, medium-grained, samples.*

Formation factor versus borehole length

Data are presented both for the laboratory measurements (Figure 3-6) and for the in situ measurements (Figure 3-7). For the in situ measurements, a selection of the data has been done so that only measurements are included that have a correspondence with a laboratory resistivity of a sample taken at the same location. A comparison indicates that the in situ measurements give a considerably lower formation factor than the corresponding laboratory measurements. Furthermore, for the laboratory resistivity measurements one can observe a tendency of increasing formation factor with increasing borehole depth. No such increase can be observed for the in situ results, which could be interpreted as sampling causing stress release of the rock samples and a following "opening up" of the pores. According to this interpretation, the stress release of the laboratory samples should cause an overestimation of the porosity and the diffusivity.

However, a slight contradiction to this interpretation is that no tendency of increased porosity with increased sampling depth can be observed for borehole KFM02A and that the general correlation of increasing porosity and diffusivity with sample depth is rather poor. (cf Figure 3-9 and 3-10). Furthermore, the ratios of laboratory and in situ formation factor (cf Table 3-5) are quite different between the boreholes KM01A and KFM02A; this difference being stronger than the slight difference observed with increasing sample depth. A possible explanation for the different ratios of the different boreholes is that rock stress is higher for the borehole KFM01A than KFM02A. The KFM01A drill-core would therefore be more influenced by stress release than the corresponding KFM02A drill-core and this would thereby explain the different ratios of the laboratory and in situ measured formation factor. This explanation is also supported by the discussion in the rock mechanic programme of the Forsmark site investigation, cf Chapter 5 SDM report.

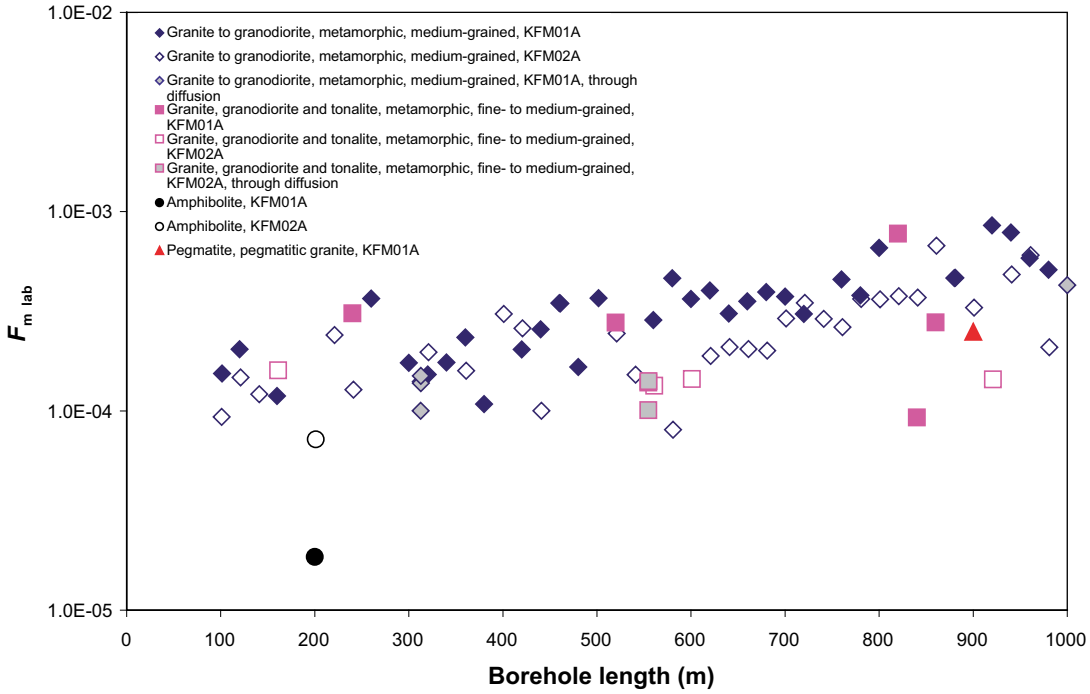

Figure 3-6. *Formation factor measured with electrical resistivity in the laboratory versus the borehole length, i.e. the position in the borehole where the sample has been taken. Comparisons are made to samples where the formation factor has been measured with through diffusion experiments.*

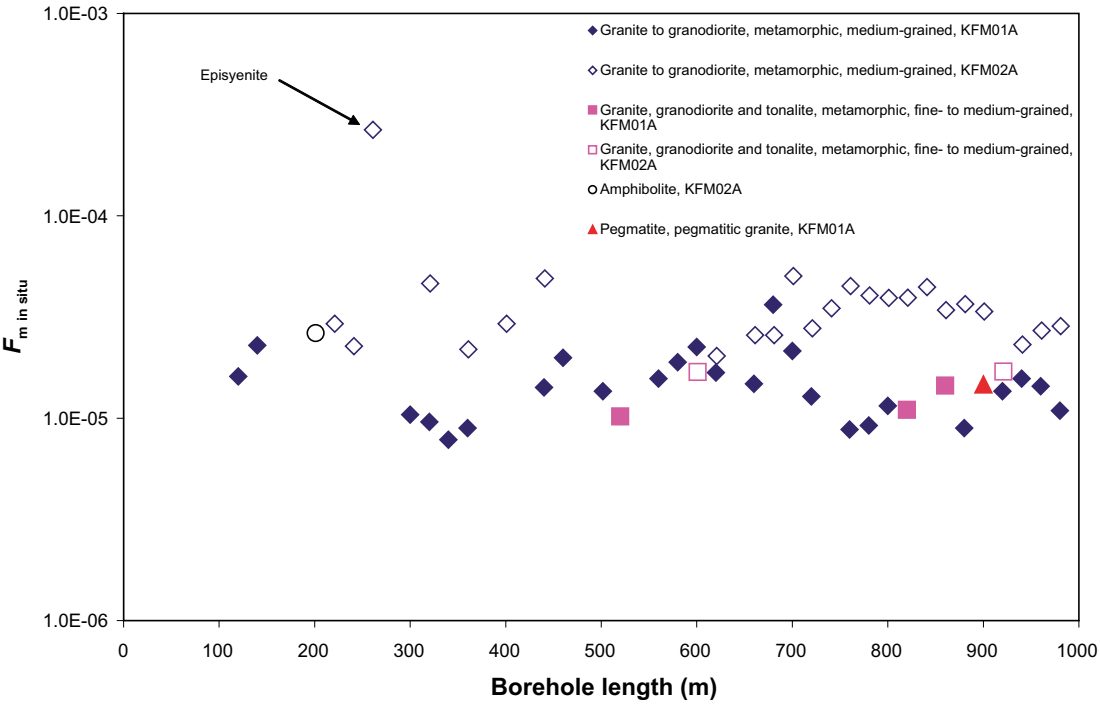

Figure 3-7. *Formation factor measured with electrical resistivity in situ versus the borehole length.*

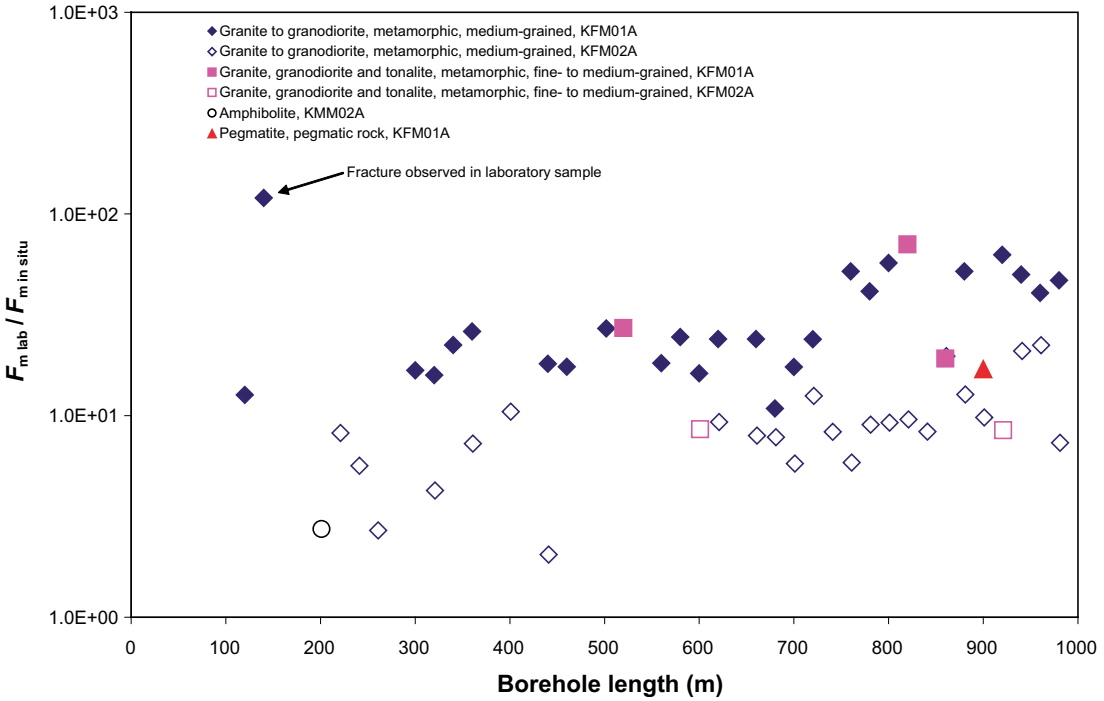

Figure 3-8. *Ratio of the formation factor measured in the laboratory and in situ with electrical resistivity versus the borehole length.*

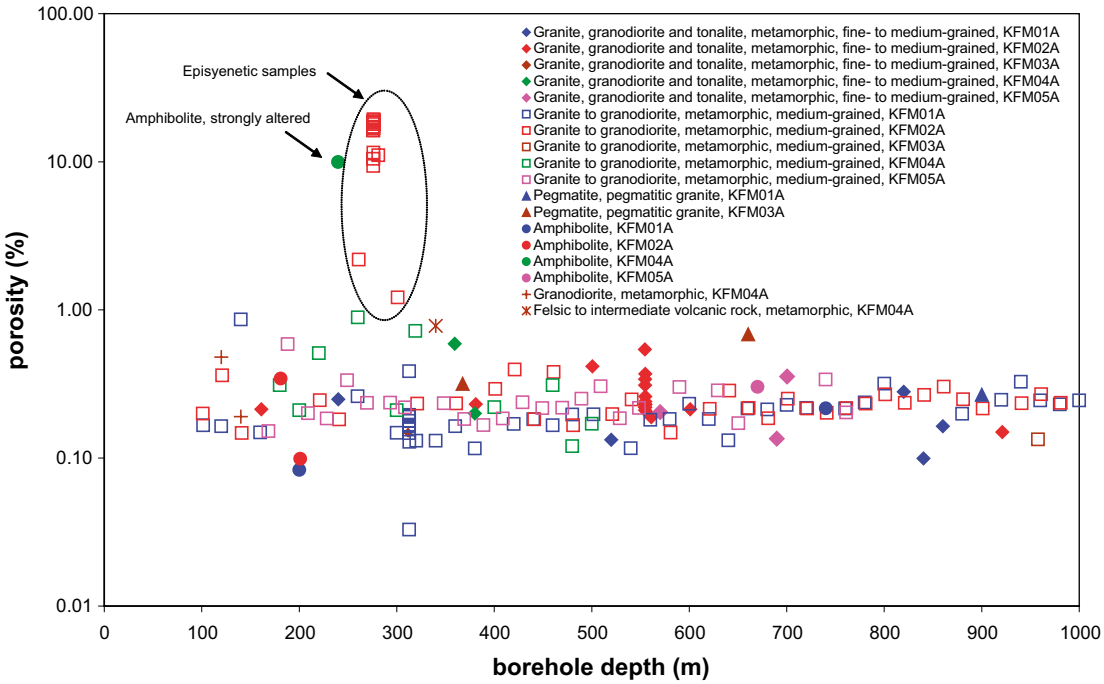

Figure 3-9. *Porosity, measured in the laboratory using the water saturation method, versus the borehole length.*

Furthermore, in Section 6.2 of the SDM report, comparisons are made of the characteristics of the P-wave measurements of the drill cores and the corresponding formation factor and porosity measurements. It is indicated that a good correlation of increased P-wave velocity and increased formation factor can be observed for the results of the drill cores; a further indication of sample disturbance caused by stress release of the drilled samples.

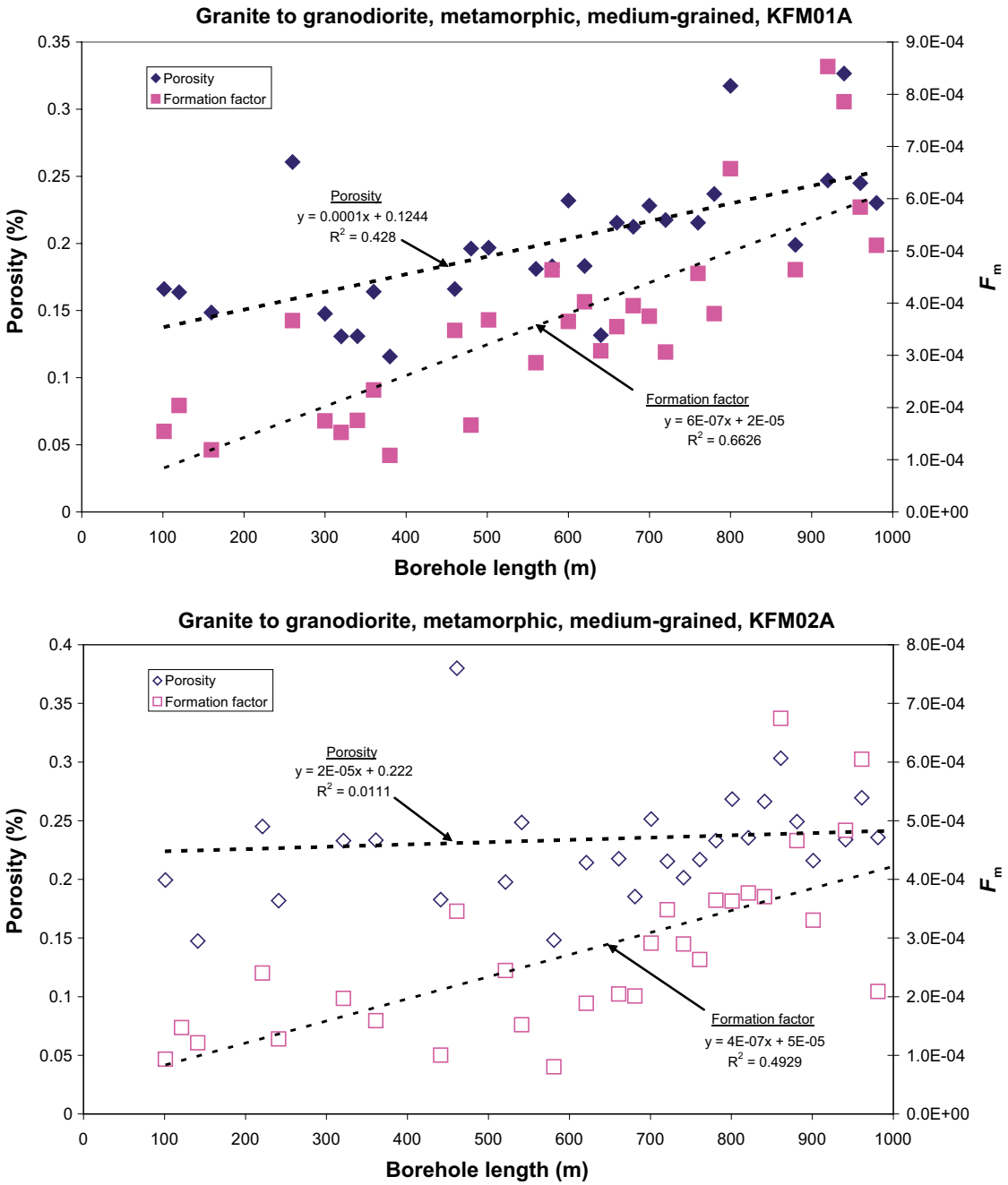

Figure 3-10. *Porosity and formation factor (lab) co-plotted as a function of sample depth. Only Granite to granodiorite, metamorphic, medium-grained, samples without visual cracks and strong alterations has been selected for this presentation.*

Table 3-4. Summary of formation factors for some of the Forsmark rock types. Mean value ± one standard deviation of experimental data set; in italics mean value, standard deviation of log_{10} of experimental data set.

Method	Granite, granodiorite and tonalite, metamorphic, fine- to medium-grained (101051)	Granite to granodiorite, metamorphic, medium-grained (101057)	Granite to granodiorite, metamorphic, medium-grained, episyenite (101057)	Pegmatite, pegmatitic granite (101061)	Amphibolite (102017)
HTO through-diffusion	(1.3±0.2)E–4	(1.9±1.3)E–4	5.9E–3	Pending	(> 1.2E–5)[1]
Log-normal distribution	*–3.90,0.08*	*–3.78,0.24*	*–2.23*	Pending	> *–4.94*[1]
Electrical resistivity, lab	(2.9±2.3)E–4	(3.2±1.7)E–4	Pending	2.5E–4	> 4.5E–5
Log-normal distribution	*–3.63,0.30*	*–3.56,0.24*	Pending	*–3.60*	> *–4.44*
Electrical resistivity, in situ	(1.2±0.2)E–5	(2.4±1.3)E–5	Pending	1.5E–5	2.6E–5
Log-normal distribution	*–4.93,0.08*	*–4.68,0.24*	Pending	*–4.83*	*–4.58*

[1)] Steady state diffusion rate not reached, only minimum diffusion rate evaluated.

Table 3-5. Results of formation factors, compared on borehole basis. Results are given for the Granite to granodiorite, metamorphic, medium-grained samples and are compared based on the results from the boreholes KFM01A and KFM02A and also as the average of both of them. Mean value ± one standard deviation of experimental data set; in italics mean value, standard deviation of log_{10} of experimental data set.

Method	Both boreholes	KFM01A	KFM02A
HTO through- diffusion	(1.9±1.3)E–4	(1.9±1.3)E–4	Pending
Log-normal distribution	*–3.78,0.24*	*–3.78,0.24*	Pending
Electrical resistivity, lab	(3.2±1.7)E–4	(3.6±1.9)E–4	(2.8±1.5)E–4
Log-normal distribution	*–3.56,0.24*	*–3.50,0.24*	*–3.61,0.24*
Electrical resistivity, in situ	(2.4±1.3)E–5	(1.5±0.6)E–5	(3.4±0.9)E–5
Log-normal distribution	*–4.68,0.24*	*–4.86,0.17*	*–4.49,0.12*
$F_{lab}/F_{in\ situ}$ resistivity measurement	20±16	30±16	10±5

Formation factor, influence of rock type

Comparing results of the different rock types, a slight tendency can be observed of the Granite to granodiorite, metamorphic, medium-grained rock type having slightly higher formation factor than the Granite, granodiorite and tonalite, metamorphic, fine- to medium-grained rock type. This is not unexpected since a more fine grained rock type is likely to be less diffusive than a less fine grained. However, one should keep in mind that the difference is not very large and that there is a large spread within the samples of each of these rock types.

The Amphibolite samples are indicated to have lower formation factor than the other rock types and the highly porous Granite to granodiorite, metamorphic, medium-grained (episyenite) has a larger formation factor. This is expected from the texture of the rock

types but since the number of measurement of this rock types are so low, the values are very uncertain. The same is valid for Pegmatite, Pegmatic rock which base on the very few available measurements has been indicated to have a formation factor in the range of the two major rock types.

3.3 Sorption

3.3.1 BET surface area

Since the adsorption of radionuclides is taking place on the surfaces of the rock material, the quantification of available surface areas is an important estimation of the sorption capacity of the rock material. For example, different ferric oxides have significant surface areas and have been shown to be a highly adsorbing mineral for cations that adsorb with surface complexation, see, e.g. /Jakobsson 1999/. Furthermore, presence of clay minerals (as a group identified as a significant potential sink for Cs^+) will also cause increased surface areas in the measurements on rock samples.

Although at this stage no method is available for establishing a quantitative relationship between specific surface areas and sorption parameters, results of BET surface area measurements are included in the retardation model as qualitative data important for the understanding of the sorption processes.

BET measurements have been performed on site-specific materials according to the ISO 9277 standard method. Two types of measurements have so far been performed for the Forsmark site specific material:

1. For samples taken from drill core, crushing and sieving has been performed. The size fractions 63–125 µm and 2–4 mm was measured in duplicate samples for each fraction. Furthermore, an extrapolation according to the methods described in Equation 3-3 was performed in order to obtain the inner surface BET area of the samples. The results of these measurements are given in Table 3-6.
2. For natural fracture samples, scraping of the fracture surfaces was performed and the < 125 µm fraction was isolated through sieving of the scraped material and measured in duplicate samples. The results of these measurements are given in Table 3-7.

Table 3-6. Measured BET surface area for the fractions 0.063–0.125 mm and 1–2 mm presented together with the result of an extrapolation of the results in order to obtain an inner surface area (concept equivalent to the concept in the K_d extrapolation, cf Equation 3-3).

Borehole	Location	Remarks	BET (m^2/g) (63–125 µm)	±	BET (m^2/g) (2–4 mm)	±	BET (m^2/g) inner surface model	±
Granite to granodiorite, metamorphic, medium-grained (101057)								
KFM01A	103.46–103.65		0.20	0.01	0.024	0.022	0.019	0.012
KFM01A	312.20–312.50		0.17	0.02	< 0.006		< 0.01	
KFM01A	487.10–487.50		0.16	0.05	0.047	0.004	0.043	0.025
KFM01A	703.25–703.45		0.095	0.007	0.012	0.004	0.0093	0.0044
KFM01A	908.18–908.36		0.12	0.06	0.030	0.001	< 0.06	
KFM03A	536.47–536.67		0.23	0.03	0.013	0.003	< 0.02	
KFM04A	694.80–695.00		0.16	0.01	0.017	0.008	0.012	0.005
KFM02A	243.50–243.70	Altered	0.77	0.01	0.20	0.01	0.18	0.01

Borehole	Location	Remarks	BET (m^2/g) (63–125 µm)	±	BET (m^2/g) (2–4 mm)	±	BET (m^2/g) inner surface model	±
KFM02A	275.22–275.45	Episyenetic	1.58	0.01	0.27	0.02	0.23	0.01
Granite, granodiorite and tonalite, metamorphic, fine- to medium-grained (101051)								
KFM01A	520.88–521.00		0.13	0.01	0.014	0.013	0.010	0.009
KFM02A	552.00–552.23		0.34	0.01	0.041	0.01	0.031	0.005
KFM02A	915.53–915.70		0.17	0.01	0.015	(single sample)	< 0.025	
KFM03A	311.01–311.21		0.32	0.01	0.022	0.003	0.013	0.001
Pegmatite, pegmatitic granite (101061)								
KFM03A	367.52–367.72		0.23	0.01	0.027	0.004	0.020	0.005
KFM03A	660.18–660.39		0.31	0.02	0.052	0.005	0.043	0.009
Tonalite and granodiorite, metamorphic (101054)								
KFM03A	242.93–243.13		0.27	0.03	0.042	0.009	0.035	0.017
Rim zone material, zone 1 type								
KFM01B	47.90–48.00		3.62	0.10	1.98	0.06	1.93	0.06

Table 3-7. Measured BET surface area for rock materials scraped off from fracture samples and the < 125 µm size fraction isolated by sieving.

Borehole	Location	Remarks	BET (m2/g) (< 125 µm)	±
Fracture material, zone 2 type				
KFM01A	418.29–418.43		3.85	0.23
KFM05A	627.85–628.00	Hydraulically conductive zone, brecciated	2.66	0.29
Hydraulically conductive fracture zone in diorite/gabbro				
KFM03A	643.80–644.17		10.3	0.2
Hydraulically conductive zone				
KFM04A	414.20–414.40		1.61	0.61

A general observation is that comparatively high BET surface areas can be found for materials associated with fractures and fracture zones.

3.3.2 Sorption data

The process “sorption” is here defined as the adsorptive interaction of radionuclides with the surfaces of the rock material. In the somewhat simplified approach taken in this work, sorption is considered to be:

- Linear (i.e. no concentration effect on the sorption).
- Fast and reversible compared to the considered time perspective (no chemical kinetic effects are addressed for the sorption processes).

The concept used for the sorption processes is the same as described in the “laboratory strategy report” /Widestrand et al. 2003/. This means that the source of sorption data will

be batch laboratory experiment performed using crushed and sieved rock material. The results from the measured distribution of tracer between the rock and water phase will be interpreted as:

- Adsorption of the tracers on the outer surfaces of the rock material, determined by the surface sorption parameter, K_a (m).
- Adsorption of the tracers on the inner surfaces of the rock material, determined by the volumetric sorption parameter, K_d (m^3/kg).

In the considered transport concept, the K_a parameter is used only to estimate the minor part of tracer retention that takes place via the sorption on the fracture walls, and is thus of less importance. The major part of the retention is caused by the diffusion of the radionuclides into the rock matrix and the subsequent sorption on the inner surfaces of the rock material.

The evaluation of the batch sorption experimental results to sorption parameters is done according to:

$$R_d = K_d + \frac{6K_a}{d_p \rho} \qquad (3\text{-}3)$$

where R_d (m^3/kg) is the measured tracer distribution between solid and liquid phases, d_p (m) is the average particle diameter, and ρ (kg/m^3) is the rock density. A graph of R_d versus $1/d_p$ gives an intercept corresponding to the K_d value, and a slope corresponding to 6 K_a/ρ. This concept of evaluation implies the following assumptions:

- Perfect spherical form of the crushed rock particles.
- The size distributions within each particle diameter interval can be represented by the mean of that interval.

Since there is no established method available for the validation of these assumptions, uncertainty in the resulting sorption has to be acknowledged, although this uncertainty can not be quantified.

Aspects of import of Finnsjön sorption data to the retardation model

Since no Forsmark site specific batch sorption data were available, alternative ways of importing data to the retardation model had to be investigated. One possible approach would be to import sorption data obtained from laboratory experiment done using rock material from the Finnsjön site investigation area. In the Forsmark 1.1 site description, it was recommended to import diffusion data from Finnsjön investigation since geographical data of the rock samples could be obtained and that the methods applied in these investigations were considered to be very similar to the methods in the corresponding SKB method description for diffusivity determination (SKB MD 540.001). For the sorption data, it was considered that the available works had shortage in the descriptions of the geographic origin of the rock samples, had lack of sophisticated geological description and/or applied experimental methods that deviated significantly from the SKB method description for batch sorption determination (SKB MD 540.002).

Since 1.1 version, a better geological and hydrogeochemical description has been obtained and is also applied in this 1.2 version and has also been the basis for the set-up of the on-going laboratory batch sorption experiments with site specific Forsmark material. Looking through the available Finnsjön sorption data, it has been concluded that none of these work are sufficiently similar to the on-going batch sorption experiment. It has therefore been decided to not make any effort to use Finnsjön sorption data as Forsmark site specific data in this 1.2 site description version and instead use a generic sorption database.

4 Development of retardation model

In accordance with the concept proposed by /Widestrand et al. 2003/, the retardation model should consist of tables in which the geological description and the selected transport parameters for each unit (rock mass or fracture/fracture zone), where retardation of radionuclides can take place, are given.

4.1 Methodology

The developed retardation model consists of two sections, one for the major rock types and one for the fractures and fracture zones. In the first section, the retention characteristics of the major rock types, i.e. rock matrix interaction parameters, are described. The second section provides a description of the retardation in the water-conducting fractures and fracture zones.

This section lists the parameters for the different sections and gives the motivations for the data selections that have been made.

4.1.1 Rock mass

According to the retention concept applied in the present work (cf Section 1.2 and Chapter 3), the retardation of radionuclides in the rock matrix can be described using the following parameters:

- ***Rock matrix porosity,*** θ_m ***(–):*** The results from the water saturation porosity measurements on site-specific rock materials have been selected in this work (cf Table 3-1). A log-normal distribution has been considered to describe the system somewhat better (although not perfectly) than a normal distribution, and has therefore been selected for the representation.
- ***Rock matrix formation factor,*** F_m ***(–):*** This parameter is used to multiply literature values of the radionuclide-specific free diffusivities in water (D_w (m^2/s); tabulated, e.g. by /Ohlsson and Neretnieks 1997/) to obtain the effective diffusivities, D_e (m^2/s), for the different radionuclides. Based on the indication of disturbances in the laboratory samples due to stress release, it has been decided to use the formation factors obtained from in situ electrical resistivity measurements. However, an existence of a conceptual uncertainty based on lack of knowledge of the pore liquid composition is acknowledged as a potential source of additional uncertainty. Nevertheless, it has in this stage been decided to consider any sample disturbances due to stress release as a potentially larger error source. As for the porosity data, a log-normal distribution has been chosen for the representation of the uncertainty of the measured data.
- ***Rock matrix sorption coefficient,*** K_d ***(m^3/kg):*** No site specific sorption coefficients are available for this 1.2 version of the Forsmark site description so this part of the retardation model will be pending.

4.1.2 Fractures and fracture zones

The present retention concept proposed by /Widestrand et al. 2003/ shall produce retardation models for the fractures and fracture zone types by describing and quantifying the retention properties of the different layers of geological materials present in and in the immediate vicinity of the fractures/fracture zones. The geological materials in the fractures and fracture zones could consist of, e.g. gouge, fracture coating, mylonite and altered wall rock. In the retardation modelling, attempts will be made to give the following parameters for the different layers:

- thickness,
- porosity,
- formation factor (to be used in calculations of the diffusivities of the different radionuclides),
- sorption parameters, i.e. surface distribution coefficients, K_a (m), and/or volumetric distribution coefficients, K_d (m^3/kg),
- mineral contents and, if possible, grain sizes.

In addition, the following data on each particular fracture type will be given:

- abundance (percentage) of the fracture type, i.e. a quantification of for how large portion of the entire fracture class the given description is valid,
- transmissivity interval observed for this particular fracture or fracture zone type,
- preferential direction (if any).

In the F1.2 site description, an identification and quantitative description of different fracture types is presented, whereas fracture zone types cannot be identified due to the limited data available. The limited amount of data also implies that some parameter values are missing in the tables describing the identified fracture types.

4.2 Retardation model

4.2.1 Rock mass

The geological model is based on rock domains, whereas the sampling for the transport programme is based on rock types and mainly focused on the major rock type; granite (to granodiorite), metamorphic, medium-grained and some minor rock types (listed below). The sample collection represents both fresh and altered samples of these rock types. The quantity of different rock types in each of the cored boreholes drilled during the site investigation programme is summarised in Table 4-1.

Major rock type:

- Granite (to granodiorite), metamorphic, medium-grained (101057). Dominate strongly in all cored boreholes.

Minor rocks types integrated in the retardation model:

- Granodiorite, tonalite and granite, metamorphic, fine- to medium-grained (rock code 101051, group C). Occur as lenses or dykes in group A and B rock types, relatively frequent and regularly distributed in all the boreholes. Of special interest because of it's relatively high content of biotite which possible will effect the sorption properties.
- Tonalite to granodiorite, metamorphic (101054) – minor part of group B rock types. Dominating rock type in the rock domains RFM17 and RFM18.
- Pegmatite, pegmatitic granite (101061) – small but regularly distribution in all boreholes also very frequent in KFM03B.
- Amphibolite (102017) – occur as dykes and irregular intrusions in group B rock types, present in all cored boreholes.
- Episyenite – hydrothermally altered, porous variant of the major rock type (101057) and to a smaller extent fine- to medium-grained granodiorite, tonalite and granite (101051). Although it just has been found as zones in KFM02A the extent in the area is unknown.

Table 4-2 present the selected transport parameters for the fresh and altered rock types. The percentages quantify the portions of the rock types that are altered; they are estimated from data in the F1.2 geological description /SKB 2005a; Chapter 5/, and only the classes medium and strong alteration have been considered.

Table 4-1. Proportions of different rock types that are greater than 1 m in borehole length in the cored boreholes. /Chapter 5 Forsmark SDM1.2, SKB 2005a/.

Code (SKB)	Composition and grain size	KFM01A	KFM01B	KFM02A	KFM03A	KFM03B	KFM04A	KFM05A
103076	Felsic to intermediate volcanic rock, metamorphic	No occurrence > 1 m	No occurrence > 1 m	No occurrence > 1 m	No occurrence > 1 m	No occurrence > 1 m	4.2%	0.3%
108019	Calc-silicate rock (skarn)	0.2%	No occurrence > 1 m	No occurrence > 1 m	No occurrence > 1 m	No occurrence > 1 m	No occurrence > 1 m	No occurrence > 1 m
102017	Amphibolite (group C)	1.9%	0.3%	4.1%	1.9%	8.5%	2.8%	3.4%
101054	Tonalite and granodiorite, metamorphic (group B)	No occurrence > 1 m	No occurrence > 1 m	No occurrence > 1 m	4.2%	No occurrence > 1 m	No occurrence > 1 m	No occurrence > 1 m
101056	Granodiorite, metamorphic	No occurrence > 1 m	No occurrence > 1 m	No occurrence > 1 m	No occurrence > 1 m	No occurrence > 1 m	10.8%	No occurrence > 1 m
101057	Granite (to granodiorite), metamorphic, medium-grained (group B)	85.3%	92.6%	79.5%	74.8%	50.3%	68.3%	89.2%
101051	Granodiorite, tonalite and granite, metamorphic, fine- to medium-grained (group C)	10.0%	6.1%	14.3%	9.9%	1.2%	10.5%	5.0%
101061	Pegmatitic granite, pegmatite (group D)	1.4%	1.0%	0.9%	6.8%	38.7%	2.3%	1.2%
111058	Granite, fine- to medium-grained	1.2%	No occurrence > 1 m	1.2%	2.4%	1.3%	1.1%	0.8%
No information		No occurrence > 1 m	No occurrence > 1 m	No occurrence > 1 m	No occurrence > 1 m	No occurrence > 1 m	No occurrence > 1 m	0.1%

Table 4-2. Suggested transport parameters (water saturation measured porosity and in situ electrical resistivity measured formation factor) for the common rock types at the Forsmark subarea. However, one should for PA purposes be aware of a possible over-estimation of these parameters caused by sample disturbances. Mean value, standard deviation of log_{10} of experimental data set.

Rock type (SKB code)	Porosity (vol %)	Formation factor (–)
Granite to granodiorite, metamorphic, medium-grained (101057).	–0.68,0.15	–4.68,0.24
Granite to granodiorite, metamorphic, medium-grained (101057), episyenetic samples.	1.05,0.36	–2.23 A
Granite, granodiorite and tonalite, metamorphic, fine- to medium-grained (101051).	–0.64,0.17	–4.93,0.08
Pegmatite, pegmatic granite (101061).	–0.41,0.22	–4.83
Amphibolite (101217).	–0.75,0.28	–4.58
Granodiorite metamorphic (101056).	–0.52,0.28	Pending
Felsic to intermediate volcanic rock, metamorphic (103076).	–0.11	Pending

[A)] Based on through diffusion experiment result.

4.2.2 Fractures

The following simplifications and quantitative estimates are used as a basis for the identification and parameterisation of different fracture types:

Chlorite is present in 70–80% of the open fractures in KFM01A–KFM06A. Calcites are often found in varying amounts in the chlorite coated fractures but are not always present. Clay minerals are found in 2–18% of the open fractures. X-ray identification shows, however, that corrensite (swelling mixed layer clay) are present in many of the open chlorite coated fractures so the frequency of clay minerals from the core mapping is probably un underestimate. Laumontite + calcite ± chlorite/corrensite is also common coating in open fracture (mostly steep fractures usually trending NE). It is however difficult to determine whether these fractures are originally open or sealed. This means that the frequency of open, laumontite coated fractures are very uncertain varying from < 1% to 19% in boreholes KFM01A to KFM06A. The large variation is also a product of the locations and directions of the boreholes. Thin but continuous coatings of euhedral quartz crystals are found in many reactivated fractures. This fracture type also carries calcite and often pyrite.

According to the presently available data, the presence of different fracture coatings cannot be related to specific rock types. This is important for the application of the identified fracture types in transport models.

Concerning the host rock only a minor portion of the fractures are accompanied by altered wall rock < 10% of the open fractures according to the core logging. If considering the nearest cm to the fracture only, this is probably an underestimation, especially for the fractures with hydrothermal minerals like epidote, prehnite and laumontite as most of the fracture coatings documented by thin sections show hydrothermal alteration /Sandtröm et al. 2004/

Generalising the information from the core mapping and the more detailed fracture mineral studies, the following quantification and description of different fracture types is suggested:

A. 50% have chlorite ± calcite ± hematite as fracture coating (max 0.5 mm thick on each side) and fresh wall rock.

B. 10% have chlorite + clay minerals (± epidote, prehnite or calcite) as fracture coating (max 1 mm thick on each side). All of these fractures have altered wall rock > 3 cm (on each side of the coating).

C. 15% have chlorite ± epidote ± prehnite as coating (max 0.5 mm thick on each side); all of these fractures have altered wall rock wall rock ca.1 cm on each side of the coating*.

D. 15% have laumontite +chlorite + calcite as fracture coating (max 0.5 mm thick on each side); all of these fractures have altered wall rock ≥ 5 cm (on each side of the coating).

E. 10% quartz + calcite + pyrite. (max 0.5 mm thick on each side) and fresh wall rock.

* The wall rock alteration is not always visible as redstaining or bleaching of feldpars but is present as alteration of plagioclase and chlorite formation due to breakdown of biotite. The density of microfractures may also be increased in the altered zone causing increased porosity.

The descriptions of the identified fracture types, including the available retardation parameters, are given in Tables 4-3 to 4-6.

Table 4-3. Retardation model for Fracture type A.

Distance	Fracture coating Max 0.5 mm	Fresh host rock 0.5 mm–
Porosity	Pending	According to Table 4-2
Formation factor	Pending	According to Table 4-2
Mineral content	Chlorite ± calcite, ± hematite	See geological description
Grain size	Pending	Pending
Portion of open structures	50%	
Transmissivity interval	Pending	
Direction	Pending	

Table 4-4. Retardation model for Fracture type B.

Distance	Fracture coating Max 1 mm	Altered wall rock 1 mm –3 cm	Fresh host rock ≥ 3 cm –
Porosity	Pending	Pending	According to Table 4-2
Formation factor	Pending	Pending	According to Table 4-2
Mineral content	Chlorite, clay minerals ± epidote ± prehnite±calcite	See geological description	See geological description
Grain size	Pending	Pending	Pending
Portion of open structures	10%		
Transmissivity interval	Pending		
Direction	Pending		

Table 4-5. Retardation model for Fracture type C.

Distance	Fracture coating Max 0.5 mm	Altered wall rock 0.5 mm –1 cm	Fresh host rock ≥ 1 cm –
Porosity	Pending	Pending	According to Table 4-2
Formation factor	Pending	Pending	According to Table 4-2
Mineral content	Chlorite, ± epidote ± prehnite	See geological description	See geological description
Grain size	Pending	Pending	Pending
Portion of open structures	15%		
Transmissivity interval	Pending		
Direction	Pending		

Table 4-6. Retardation model for Fracture type D.

Distance	Fracture coating Max 0.5 mm	Altered wall rock 0.5 mm – ≥ 1 cm	Fresh host rock ≥ 1 cm –
Porosity	Pending	Pending	According to Table 4-2
Formation factor	Pending	Pending	According to Table 4-2
Mineral content	Laumontite, chlorite, calcite, hematite	See geological description	See geological description
Grain size	Pending	Pending	Pending
Portion of open structures	15%		
Transmissivity interval	Pending		
Direction	Pending		

Table 4-7. Retardation model for Fracture type E.

Distance	Fracture coating Max 0.5 mm	Fresh host rock ≥ 0.5 mm –
Porosity	Pending	According to Table 4-2
Formation factor	Pending	According to Table 4-2
Mineral content	Chlorite, calcite, clay minerals	See geological description
Grain size	Pending	Pending
Portion of open structures	10%	
Transmissivity interval	Pending	
Direction	Pending	

4.2.3 Deformation zones

It is not yet possible to give a retardations model for the deformation zones.

4.3 Application of the retardation model

Tables 4-1 and 4-2 provide a basis for parameterisation of the rock domains RSMA01, RSMB01 and RSMC01. The parameterisation of each rock domain could range from a simple selection of a single parameter value for the dominant rock type in that domain to, for instance, volume averaging using data for fresh or altered rock, or both. For the diffusion parameters of the major rock types, statistical distributions are given that can be used as a basis for stochastic parameterisation of transport models.

However, no specific recommendations on the selection of data from the retardation model are given here. This implies that the present model does not provide detailed guidelines on how to "dress" the geological model with transport parameters using the parameters in the retardation model. At this stage of model development, the retardation model should be viewed as a presentation of the interpreted site-specific information on retardation parameters, intended to provide a basis for the formulation of alternative parameterisations within the Safety Assessment modelling.

The quantitative descriptions of the identified fracture types, including the available retardation parameters, are given in Tables 4-3 to 4-6. The fracture types in the present retardation model could be used as a basis for modelling radionuclide transport along flow paths in the fractured medium. However, the presented model could also be viewed as primarily proposing a basic structure, for discussion and further development, which from the viewpoint of numerical transport modelling will become more useful when more data is at hand.

Concerning the parameterisation of flow paths in transport models, it should also be noted that at present there is no data supporting, for instance, quantitative correlations between fracture types and hydraulic properties. Furthermore, it could be observed that the present data indicate that the presence of different fracture coatings cannot be related to specific rock types.

No identification or description of fracture zone types is given in the present model. However, the available information and indications related to fracture zones are described in Section 4.2.3.

4.4 Evidence from process-based modelling

As discussed in Section 1.2.2, alternative retention processes and process models are considered within the site descriptive transport modelling, so far mainly in the form of process-based sorption models. It is expected that the results of this modelling will be useful for supporting, or providing alternatives to, the K_d-based sorption model, regarding actual parameter values as well as for the understanding of the site-specific sorption processes in general. However, no results that can be used for these purposes are presently available.

4.5 Evaluation of uncertainties

General discussions on the uncertainties related to the site-descriptive transport model are given in the transport modelling guidelines /Berglund and Selroos 2004/ and in the F1.1 modelling report /SKB 2004/. Similar to the other geoscientific disciplines, spatial variability is considered an important potential source to uncertainty in the modelling of transport properties. Quantitative results from previous studies on Äspö /Byegård et al. 1998, 2001, Löfgren and Neretnieks 2003, Xu and Wörman 1998/, demonstrating spatial variability along flow paths and within the matrix, are briefly summarised in /SKB 2004/.

The main uncertainties identified in the F1.1 modelling were related to the absence of site-specific transport data. As described in the present report, this uncertainty has been partly resolved in the F1.2 model, although significant data gaps still remain. In particular, no site-specific sorption parameters have been available for the F1.2 modelling. Furthermore, the available data are insufficient for establishing quantitative relations between transport parameters and other properties of fractures and fracture zones, e.g. lengths, orientations and hydraulic properties. The uncertainties relevant for present description of transport properties can be categorised as follows:

- Uncertainties in the data and models obtained from other disciplines, primarily Geology and Hydrogeochemistry.
- Uncertainties in the interpretations and use of data and models from other disciplines, i.e. in interpretations of the relations between transport properties and various underlying properties, and the simplifications made when identifying and parameterisation of “typical” materials and fractures.

- Data uncertainties related to measurements and spatial variability of transport parameters, including the "extrapolation" of small-scale measurements to relevant model scales.
- Conceptual uncertainties related to transport-specific processes and process models.

This model provides quantitative information on transport data uncertainties only. Uncertainty ranges, in most cases taken directly from the experimental data, are given in the data tables above. Essentially, these ranges incorporate both random measurement errors and the spatial variability associated with the particular dataset.

The uncertainties introduced by the inputs from other disciplines and by the "expert judgement" utilised to interpret and use these data have not been addressed in the transport description. Whereas the uncertainties in the descriptions devised by Geology and Hydrogeochemistry are discussed in the F1.2 SDM report /SKB 2005a/, Chapters 5 and 9, respectively, no attempt has been made to formulate alternative interpretations or otherwise address the "expert judgment" aspects of the work. It can be noted, however, that the differences in parameter values between, e.g. different rock types give some indications on the possible ranges of these uncertainties.

Regarding the uncertainties related to spatial variability and scale, it may be noted that all measurements providing data to the retardation model mainly have been obtained in the laboratory, on a millimetre- to centimetre-scale. The proper means of "upscaling" these parameters is by integrating them along flow paths in groundwater flow models, implying that the scale of the flow model is the relevant model scale. The approach is here to present the data on the measurement scale, thereby providing a basis for further analysis in connection with the numerical flow and transport modelling.

5 Implications for further studies

A complication is that considerable systematic differences are obtained for the in situ formation factor measurements compared to corresponding laboratory measured formation factors. Both methods involves methods uncertainties; for the in situ measurements there are only very limited information concerning the pore liquid composition and laboratory samples are indicated to have been exposed for stress release. Further information is therefore needed, at least for a more correct quantification of the uncertainty involved with the different methods.

The porosity measurements indicate that there is a large spread in data, even for samples taken very close to each other. In forthcoming site descriptions it is foreseen that PMMA measured porosity data will be available which will make it possible to address sample heterogeneity of the samples.

A considerable drawback is, furthermore, that no addressing of site specific sorption data is done within this site description model. Since work in this area is on-going, it can be foreseen that a better description of this topic will be possible to perform in forthcoming site descriptions of Forsmark.

6 References

Andersson P, Byegård J, Dershowitz B, Doe T, Hermanson J, Meier P, Tullborg E-L, Winberg A, 2002. Final report of the TRUE Block Scale projekt 1. Characterisation and model development. SKB TR-02-13. Svensk Kärnbränslehantering AB

Berglund S, Selroos J-O, 2004. Transport properties site descriptive model – Guidelines for evaluation and modelling. SKB R-03-09, Svensk Kärnbränslehantering AB.

Brunauer S, Emmett P H, Teller E, 1938. Adsorption of gases in multimolecular layers. J Amer Chem Soc 60: 309–319.

Byegård J, Johansson H, Skålberg M, Tullborg E-L, 1998. The interaction of sorbing and non-sorbing tracers with different Äspö rock types – Sorption and diffusion experiments in the laboratory scale. SKB TR 98-18, Svensk Kärnbränslehantering AB.

Byegård J, Widestrand H, Skålberg M, Tullborg E-L, Siitari-Kauppi M, 2001. Complementary investigation of diffusivity, porosity and sorptivity of Feature A-site specific geological material. SKB ICR-01-04. Svensk Kärnbränslehantering AB.

Dershowitz W, Winberg A, Hermanson J, Byegård J, Tullborg E-L, Andersson P, Mazurek M, 2003. Äspö Hard Rock Laboratory. Äspö Task Force on modelling of groundwater flow and transport of solutes – Task 6C – A semi-synthetic model of block scale conductive structures at the Äspö HRL. SKB IPR-03-13. Svensk Kärnbränslehantering AB.

Eliasson T, 1993. Mineralogy, geochemistry and petrophysics of red coloured granite adjacent to fractures. SKB TR-93-06, Svensk Kärnbränslehantering AB.

Jakobsson, 1999. Mesurement and modelling using surface complexation of cation (II to IV) sorption onto mineral oxides, Thesis, Chalmers University of Technology, Department of Nuclear Chemistry, Göteborg, Sweden.

Johansson H, Byegård J, Skarnemark G, Skålberg M, 1997. Matrix diffusion of some alkali and alkaline earth metals in granitic rock. Mat. Res. Soc. Symp. Proc. 465: 871–878.

Löfgren M, Neretnieks I, 2003. Formation factor logging by electrical methods. Comparison of formation factor logs obtained in situ and in the laboratory. J. Contam. Hydrol. 61: 107–115.

Löfgren M, Neretnieks I, 2005. Formation factor logging in-situ by electrical methods in KFM01A and KFM02A. Measurements and evaluation of methodology. SKB P-05-29. Svensk Kärnbränslehantering AB

Ohlsson Y, Neretnieks I, 1997. Diffusion data in granite – Recommended values. SKB TR-97-20, Svensk Kärnbränslehantering AB.

Poteri A, Billaux D, Dershowitz W, Gomez-Hernandez JJ, Cvetkovic V, Hautojärvi A, Holton D, Medina A, Winberg A (ed.), 2002. Final report of the TRUE Block Scale project. 3. Modelling of flow and transport. SKB TR-02-15. Svensk Kärnbränslehantering AB.

Sandström B, Savolainen M, Tullborg E-L 2004. Fracture mineralogy. Results from fracture minerals and wall rock alteration in boreholes KFM01A, KFM02A, KFM03A and KFM03B. Forsmark site investigation. SKB P 04-149, Svensk Kärnbränslehantering AB.

SKB, 2004. Preliminary site description. Forsmark area – version 1.1. SKB R-04-15, Svensk Kärnbränslehantering AB.

SKB, 2005. Preliminary site description. Forsmark area – version 1.2. SKB R-05-18, Svensk Kärnbränslehantering AB.

SKB, 2005b. Hydrochemical evaluation. Preliminary site description Forsmark area – version 1.2. SKB R-05-17. Svensk Kärnbränslehantering AB

Stephens M B, Lundqvist S, Berman T, Ekström M, 2005. Bedrock mapping. Petrographic and geochemical characteristics of rock types beased on Stage 1 (2002) and Stage 2 (2003) surface data. Forsmark site investigation. SKB P-04-87, Svensk Kärnbränslehantering AB.

Stråhle A, 2001. Definition och beskrivning av parametrar för geologisk, geofysisk och bergmekanisk kartering av berget. SKB R-01-19, Svensk Kärnbränslehantering AB.

Thunehed H, 2005. Resistivity measurements on samples from KFM01A and KFM02A. Forsmark site investigation SKB P-05-26, Svensk Kärnbränslehantering

Widestrand H, Byegård J, Ohlsson Y, Tullborg E-L, 2003. Strategy for the use of laboratory methods in the site investigations programme for the transport properties of the rock. SKB R-03-20, Svensk Kärnbränslehantering AB.

Winberg A, Andersson P, Hermansson J, Byegård J, Cvetkovic V, Birgersson L, 2000. Äspö Hard Rock Laboratory. Final report on the first stage of the tracer retention understanding experiments. SKB TR-00-07. Svensk Kärnbränslehantering AB.

Xu, S, Wörman A, 1998. Statistical Patterns of Geochemistry in Crystalline Rock and Effect of Sorption Kinetics on Radionuclide Migration. SKI Technical Report 98:41. Statens kärnkraftinspektion.

Appendix 1

Porosity data

Results of porosity measurements on samples taken for laboratory through-diffusion and batch-sorption experiments.

Table A-1. Porosity data from KFM01A.

Borehole	Secup	Seclow	Rock name	Porosity %
KFM01A	101.49	101.52	Granite to granodiorite, metamorphic, medium-grained	0.17
KFM01A	119.99	120.02	Granite to granodiorite, metamorphic, medium-grained	0.16
KFM01A	140.01	140.04	Granite to granodiorite, metamorphic, medium-grained	0.86
KFM01A	159.81	159.84	Granite to granodiorite, metamorphic, medium-grained	0.15
KFM01A	199.96	199.99	Amphibolite	0.08
KFM01A	240.01	240.04	Granite, granodiorite and tonalite, metamorphic, fine- to medium-grained	0.25
KFM01A	259.91	259.94	Granite to granodiorite, metamorphic, medium-grained	0.26
KFM01A	300.01	300.04	Granite to granodiorite, metamorphic, medium-grained	0.15
KFM01A	312.53	312.54	Granite to granodiorite, metamorphic, medium-grained	0.19
KFM01A	312.54	312.55	Granite to granodiorite, metamorphic, medium-grained	0.20
KFM01A	312.56	312.59	Granite to granodiorite, metamorphic, medium-grained	0.16
KFM01A	312.59	312.64	Granite to granodiorite, metamorphic, medium-grained	0.17
KFM01A	312.65	312.66	Granite to granodiorite, metamorphic, medium-grained	0.19
KFM01A	312.66	312.67	Granite to granodiorite, metamorphic, medium-grained	0.19
KFM01A	312.68	312.71	Granite to granodiorite, metamorphic, medium-grained	0.16
KFM01A	312.71	312.76	Granite to granodiorite, metamorphic, medium-grained	0.18
KFM01A	312.76	312.77	Granite to granodiorite, metamorphic, medium-grained	0.39
KFM01A	312.77	312.78	Granite to granodiorite, metamorphic, medium-grained	0.15
KFM01A	312.78	312.81	Granite to granodiorite, metamorphic, medium-grained	0.03
KFM01A	312.81	312.86	Granite to granodiorite, metamorphic, medium-grained	0.13
KFM01A	320.01	320.04	Granite to granodiorite, metamorphic, medium-grained	0.13
KFM01A	340.01	340.04	Granite to granodiorite, metamorphic, medium-grained	0.13
KFM01A	360.01	360.04	Granite to granodiorite, metamorphic, medium-grained	0.16
KFM01A	380.01	380.04	Granite to granodiorite, metamorphic, medium-grained	0.12
KFM01A	420.01	420.04	Granite to granodiorite, metamorphic, medium-grained	0.17
KFM01A	440.01	440.04	Granite to granodiorite, metamorphic, medium-grained	0.18
KFM01A	460.01	460.04	Granite to granodiorite, metamorphic, medium-grained	0.17
KFM01A	480.01	480.04	Granite to granodiorite, metamorphic, medium-grained	0.20
KFM01A	501.73	501.76	Granite to granodiorite, metamorphic, medium-grained	0.20
KFM01A	520.01	520.04	Granite, granodiorite and tonalite, metamorphic, fine- to medium-grained	0.13
KFM01A	539.99	540.02	Granite to granodiorite, metamorphic, medium-grained	0.12
KFM01A	560.01	560.04	Granite to granodiorite, metamorphic, medium-grained	0.18
KFM01A	580.01	580.04	Granite to granodiorite, metamorphic, medium-grained	0.18
KFM01A	600.01	600.04	Granite to granodiorite, metamorphic, medium-grained	0.23
KFM01A	620.01	620.04	Granite to granodiorite, metamorphic, medium-grained	0.18
KFM01A	640.06	640.09	Granite to granodiorite, metamorphic, medium-grained	0.13
KFM01A	659.86	659.89	Granite to granodiorite, metamorphic, medium-grained	0.22

Borehole	Secup	Seclow	Rock name	Porosity %
KFM01A	680.01	680.04	Granite to granodiorite, metamorphic, medium-grained	0.21
KFM01A	699.96	699.99	Granite to granodiorite, metamorphic, medium-grained	0.23
KFM01A	719.96	719.99	Granite to granodiorite, metamorphic, medium-grained	0.22
KFM01A	740.01	740.04	Amphibolite	0.22
KFM01A	760.01	760.04	Granite to granodiorite, metamorphic, medium-grained	0.22
KFM01A	780.01	780.04	Granite to granodiorite, metamorphic, medium-grained	0.24
KFM01A	800.01	800.04	Granite to granodiorite, metamorphic, medium-grained	0.32
KFM01A	820.01	820.04	Granite, granodiorite and tonalite, metamorphic, fine- to medium-grained	0.28
KFM01A	840.17	840.20	Granite, granodiorite and tonalite, metamorphic, fine- to medium-grained	0.10
KFM01A	860.01	860.04	Granite, granodiorite and tonalite, metamorphic, fine- to medium-grained	0.16
KFM01A	880.01	880.04	Granite to granodiorite, metamorphic, medium-grained	0.20
KFM01A	900.01	900.04	Pegmatite, pegmatitic granite	0.27
KFM01A	920.01	920.04	Granite to granodiorite, metamorphic, medium-grained	0.25
KFM01A	940.06	940.09	Granite to granodiorite, metamorphic, medium-grained	0.33
KFM01A	960.01	960.04	Granite to granodiorite, metamorphic, medium-grained	0.24
KFM01A	980.01	980.04	Granite to granodiorite, metamorphic, medium-grained	0.23
KFM01A	999.96	999.99	Granite to granodiorite, metamorphic, medium-grained	0.24

Table A-2. Porosity data from KFM02A.

Borehole	Secup	Seclow	Rock name	Porosity %
KFM02A	101.01	101.04	Granite to granodiorite, metamorphic, medium-grained	0.20
KFM02A	121.01	121.04	Granite to granodiorite, metamorphic, medium-grained	0.36
KFM02A	141.01	141.04	Granite to granodiorite, metamorphic, medium-grained	0.15
KFM02A	161.01	161.04	Granite, granodiorite and tonalite, metamorphic, fine- to medium-grained	0.21
KFM02A	181.01	181.04	Amphibolite	0.34
KFM02A	201.01	201.04	Amphibolite	0.10
KFM02A	221.01	221.04	Granite to granodiorite, metamorphic, medium-grained	0.25
KFM02A	241.01	241.04	Granite to granodiorite, metamorphic, medium-grained	0.18
KFM02A	261.01	261.04	Granite to granodiorite, metamorphic, medium-grained	2.18
KFM02A	275.93	275.94	Granite to granodiorite, metamorphic, medium-grained	9.36
KFM02A	275.94	275.95	Granite to granodiorite, metamorphic, medium-grained	16.32
KFM02A	275.95	275.98	Granite to granodiorite, metamorphic, medium-grained	17.22
KFM02A	275.99	276.04	Granite to granodiorite, metamorphic, medium-grained	17.94
KFM02A	276.04	276.05	Granite to granodiorite, metamorphic, medium-grained	10.45
KFM02A	276.05	276.06	Granite to granodiorite, metamorphic, medium-grained	16.25
KFM02A	276.06	276.09	Granite to granodiorite, metamorphic, medium-grained	18.42
KFM02A	276.10	276.15	Granite to granodiorite, metamorphic, medium-grained	18.52
KFM02A	276.15	276.16	Granite to granodiorite, metamorphic, medium-grained	11.54
KFM02A	276.16	276.17	Granite to granodiorite, metamorphic, medium-grained	16.84
KFM02A	276.17	276.20	Granite to granodiorite, metamorphic, medium-grained	19.33
KFM02A	276.20	276.25	Granite to granodiorite, metamorphic, medium-grained	19.09
KFM02A	281.01	281.04	Granite to granodiorite, metamorphic, medium-grained	11.05
KFM02A	300.96	300.99	Granite to granodiorite, metamorphic, medium-grained	1.21

Borehole	Secup	Seclow	Rock name	Porosity %
KFM02A	321.01	321.04	Granite to granodiorite, metamorphic, medium-grained	0.23
KFM02A	361.01	361.04	Granite to granodiorite, metamorphic, medium-grained	0.23
KFM02A	381.01	381.04	Granite, granodiorite and tonalite, metamorphic, fine- to medium-grained	0.23
KFM02A	401.01	401.04	Granite to granodiorite, metamorphic, medium-grained	0.29
KFM02A	420.93	420.96	Granite to granodiorite, metamorphic, medium-grained	0.40
KFM02A	440.96	440.99	Granite to granodiorite, metamorphic, medium-grained	0.18
KFM02A	460.96	460.99	Granite to granodiorite, metamorphic, medium-grained	0.38
KFM02A	481.01	481.04	Granite to granodiorite, metamorphic, medium-grained	0.17
KFM02A	500.68	500.71	Granite, granodiorite and tonalite, metamorphic, fine- to medium-grained	0.42
KFM02A	521.01	521.04	Granite to granodiorite, metamorphic, medium-grained	0.20
KFM02A	541.01	541.04	Granite to granodiorite, metamorphic, medium-grained	0.25
KFM02A	554.59	554.60	Granite, granodiorite and tonalite, metamorphic, fine- to medium-grained	0.54
KFM02A	554.60	554.61	Granite, granodiorite and tonalite, metamorphic, fine- to medium-grained	0.31
KFM02A	554.61	554.64	Granite, granodiorite and tonalite, metamorphic, fine- to medium-grained	0.23
KFM02A	554.65	554.7	Granite, granodiorite and tonalite, metamorphic, fine- to medium-grained	0.22
KFM02A	554.70	554.71	Granite, granodiorite and tonalite, metamorphic, fine- to medium-grained	0.34
KFM02A	554.71	554.72	Granite, granodiorite and tonalite, metamorphic, fine- to medium-grained	0.21
KFM02A	554.72	554.75	Granite, granodiorite and tonalite, metamorphic, fine- to medium-grained	0.22
KFM02A	554.76	554.81	Granite, granodiorite and tonalite, metamorphic, fine- to medium-grained	0.23
KFM02A	554.81	554.82	Granite, granodiorite and tonalite, metamorphic, fine- to medium-grained	0.37
KFM02A	554.84	554.85	Granite, granodiorite and tonalite, metamorphic, fine- to medium-grained	0.26
KFM02A	554.86	554.89	Granite, granodiorite and tonalite, metamorphic, fine- to medium-grained	0.23
KFM02A	554.90	554.95	Granite, granodiorite and tonalite, metamorphic, fine- to medium-grained	0.24
KFM02A	561.01	561.04	Granite, granodiorite and tonalite, metamorphic, fine- to medium-grained	0.19
KFM02A	580.89	580.92	Granite to granodiorite, metamorphic, medium-grained	0.15
KFM02A	601.01	601.04	Granite, granodiorite and tonalite, metamorphic, fine- to medium-grained	0.21
KFM02A	620.96	620.99	Granite to granodiorite, metamorphic, medium-grained	0.21
KFM02A	641.01	641.04	Granite to granodiorite, metamorphic, medium-grained	0.28
KFM02A	661.01	661.04	Granite to granodiorite, metamorphic, medium-grained	0.22
KFM02A	681.01	681.04	Granite to granodiorite, metamorphic, medium-grained	0.19
KFM02A	701.01	701.04	Granite to granodiorite, metamorphic, medium-grained	0.25
KFM02A	721.01	721.04	Granite to granodiorite, metamorphic, medium-grained	0.22
KFM02A	741.01	741.04	Granite to granodiorite, metamorphic, medium-grained	0.20
KFM02A	761.01	761.04	Granite to granodiorite, metamorphic, medium-grained	0.22
KFM02A	781.01	781.04	Granite to granodiorite, metamorphic, medium-grained	0.23
KFM02A	801.01	801.04	Granite to granodiorite, metamorphic, medium-grained	0.27
KFM02A	821.01	821.04	Granite to granodiorite, metamorphic, medium-grained	0.24

Borehole	Secup	Seclow	Rock name	Porosity %
KFM02A	841.01	841.04	Granite to granodiorite, metamorphic, medium-grained	0.27
KFM02A	861.01	861.04	Granite to granodiorite, metamorphic, medium-grained	0.30
KFM02A	881.01	881.04	Granite to granodiorite, metamorphic, medium-grained	0.25
KFM02A	901.01	901.04	Granite to granodiorite, metamorphic, medium-grained	0.22
KFM02A	921.01	921.04	Granite, granodiorite and tonalite, metamorphic, fine- to medium-grained	0.15
KFM02A	941.01	941.04	Granite to granodiorite, metamorphic, medium-grained	0.23
KFM02A	961.01	961.04	Granite to granodiorite, metamorphic, medium-grained	0.27
KFM02A	981.04	981.07	Granite to granodiorite, metamorphic, medium-grained	0.24
KFM02A	1001.01	1001.04	Granite to granodiorite, metamorphic, medium-grained	0.25

Table A-3. Porosity data from KFM03A, KFM04A and KFM05A.

Borehole	Secup	Seclow	Rock name	Porosity %
KFM03A	76.74	76.77	Pegmatite, pegmatitic granite	0.24
KFM03A	311.45	311.48	Granite, granodiorite and tonalite, metamorphic, fine- to medium-grained,	0.15
KFM03A	367.44	367.47	Pegmatite, pegmatitic granite	0.32
KFM03A	660.41	660.44	Pegmatite, pegmatitic granite	0.68
KFM03A	957.67	957.70	Granite to granodiorite, metamorphic, medium-grained	0.13
KFM04A	120.04	120.07	Granodiorite, metamorphic	0.48
KFM04A	140.03	140.06	Granodiorite, metamorphic	0.19
KFM04A	180.02	180.05	Granite to granodiorite, metamorphic, medium-grained	0.31
KFM04A	199.93	199.96	Granite to granodiorite, metamorphic, medium-grained	0.21
KFM04A	220.00	220.03	Granite to granodiorite, metamorphic, medium-grained	0.51
KFM04A	239.70	239.73	Amphibolite	9.95
KFM04A	260.00	260.03	Granite to granodiorite, metamorphic, medium-grained	0.89
KFM04A	300.04	300.07	Granite to granodiorite, metamorphic, medium-grained	0.21
KFM04A	319.09	319.12	Granite to granodiorite, metamorphic, medium-grained	0.72
KFM04A	339.83	339.86	Felsic to intermediate volcanic rock, metamorphic	0.78
KFM04A	359.18	359.21	Granite, granodiorite and tonalite, metamorphic, fine- to medium-grained,	0.59
KFM04A	379.95	379.98	Granite, granodiorite and tonalite, metamorphic, fine- to medium-grained	0.20
KFM04A	401.10	401.13	Granite to granodiorite, metamorphic, medium-grained	0.22
KFM04A	420.19	420.22	Granite, granodiorite and tonalite, metamorphic, fine- to medium-grained	1.60
KFM04A	459.93	459.96	Granite to granodiorite, metamorphic, medium-grained	0.31
KFM04A	479.93	479.96	Granite to granodiorite, metamorphic, medium-grained	0.12
KFM04A	499.91	499.94	Granite to granodiorite, metamorphic, medium-grained	0.17
KFM05A	168.34	168.37	Granite to granodiorite, metamorphic, medium-grained	0.15
KFM05A	188.03	188.06	Granite to granodiorite, metamorphic, medium-grained	0.59
KFM05A	208.82	208.85	Granite to granodiorite, metamorphic, medium-grained	0.20
KFM05A	228.13	228.16	Granite to granodiorite, metamorphic, medium-grained	0.18
KFM05A	249.03	249.06	Granite to granodiorite, metamorphic, medium-grained	0.33
KFM05A	269.66	269.69	Granite to granodiorite, metamorphic, medium-grained	0.24
KFM05A	293.11	293.15	Granite to granodiorite, metamorphic, medium-grained	0.24
KFM05A	308.55	308.58	Granite to granodiorite, metamorphic, medium-grained	0.22

Borehole	Secup	Seclow	Rock name	Porosity %
KFM05A	348.25	348.28	Granite to granodiorite, metamorphic, medium-grained	0.23
KFM05A	369.23	369.26	Granite to granodiorite, metamorphic, medium-grained	0.18
KFM05A	388.93	388.96	Granite to granodiorite, metamorphic, medium-grained	0.17
KFM05A	408.75	408.78	Granite to granodiorite, metamorphic, medium-grained	0.18
KFM05A	428.92	428.95	Granite to granodiorite, metamorphic, medium-grained	0.24
KFM05A	449.35	449.38	Granite to granodiorite, metamorphic, medium-grained	0.22
KFM05A	469.83	469.86	Granite to granodiorite, metamorphic, medium-grained	0.22
KFM05A	489.36	489.39	Granite to granodiorite, metamorphic, medium-grained	0.25
KFM05A	509.07	509.10	Granite to granodiorite, metamorphic, medium-grained	0.30
KFM05A	528.72	528.75	Granite to granodiorite, metamorphic, medium-grained	0.18
KFM05A	548.54	548.57	Granite to granodiorite, metamorphic, medium-grained	0.22
KFM05A	570.04	570.07	Granite, granodiorite and tonalite, metamorphic, fine- to medium-grained	0.20
KFM05A	590.05	590.08	Granite to granodiorite, metamorphic, medium-grained	0.30
KFM05A	629.30	629.33	Granite to granodiorite, metamorphic, medium-grained	0.29
KFM05A	650.42	650.45	Granite to granodiorite, metamorphic, medium-grained	0.17
KFM05A	669.90	669.93	Amphibolite	0.30
KFM05A	689.69	689.72	Granite, granodiorite and tonalite, metamorphic, fine- to medium-grained	0.13
KFM05A	700.28	700.31	Granite, granodiorite and tonalite, metamorphic, fine- to medium-grained	0.35
KFM05A	739.82	739.85	Granite to granodiorite, metamorphic, medium-grained	0.34
KFM05A	761.07	761.10	Granite to granodiorite, metamorphic, medium-grained	0.20

Appendix 2

Formation factors and associated porosities

Laboratory and in situ formation factors (Fm), and porosities measured on samples used in laboratory formation factor measurements.

Table A-3. Formation factor and porosity data from KFM01A.

Borehole length (m)	Porosity (%)	Formation factor Lab	Formation factor In situ	Rock description
101.49	0.17	1.54E–04		Granite to granodiorite, metamorphic, medium-grained
119.99	0.16	2.04E–04	1.61E–05	Granite to granodiorite, metamorphic, medium-grained
140.01	0.86	2.75E–03	2.29E–05	Granite to granodiorite, metamorphic, medium-grained
159.81	0.15	1.19E–04		Granite to granodiorite, metamorphic, medium-grained
199.96	0.08	1.85E–05		Amphibolite, KFM01A
240.01	0.25	3.09E–04		Granite, granodiorite and tonalite, metamorphic, fine- to medium-grained
259.91	0.26	3.66E–04		Granite to granodiorite, metamorphic, medium-grained
300.01	0.15	1.74E–04	1.04E–05	Granite to granodiorite, metamorphic, medium-grained
320.01	0.13	1.52E–04	9.58E–06	Granite to granodiorite, metamorphic, medium-grained
340.01	0.13	1.75E–04	7.83E–06	Granite to granodiorite, metamorphic, medium-grained
360.01	0.16	2.34E–04	8.94E–06	Granite to granodiorite, metamorphic, medium-grained
380.01	0.12	1.08E–04		Granite to granodiorite, metamorphic, medium-grained
420.01	0.17	2.04E–04		Granite to granodiorite, metamorphic, medium-grained,
440.01	0.18	2.57E–04	1.42E–05	Granite to granodiorite, metamorphic, medium-grained
460.01	0.17	3.48E–04	1.99E–05	Granite to granodiorite, metamorphic, medium-grained
480.01	0.20	1.66E–04		Granite to granodiorite, metamorphic, medium-grained
501.72	0.20	3.68E–04	1.36E–05	Granite to granodiorite, metamorphic, medium-grained
520.01	0.13	2.77E–04	1.02E–05	Granite, granodiorite and tonalite, metamorphic, fine- to medium-grained
560.01	0.18	2.86E–04	1.57E–05	Granite to granodiorite, metamorphic, medium-grained
580.01	0.18	4.64E–04	1.89E–05	Granite to granodiorite, metamorphic, medium-grained
600.01	0.23	3.65E–04	2.25E–05	Granite to granodiorite, metamorphic, medium-grained
620.01	0.18	4.03E–04	1.68E–05	Granite to granodiorite, metamorphic, medium-grained
640.06	0.13	3.08E–04		Granite to granodiorite, metamorphic, medium-grained
659.86	0.22	3.55E–04	1.48E–05	Granite to granodiorite, metamorphic, medium-grained
680.01	0.21	3.95E–04	3.64E–05	Granite to granodiorite, metamorphic, medium-grained
699.96	0.23	3.75E–04	2.15E–05	Granite to granodiorite, metamorphic, medium-grained
719.96	0.22	3.06E–04	1.28E–05	Granite to granodiorite, metamorphic, medium-grained
760.01	0.22	4.57E–04	8.79E–06	Granite to granodiorite, metamorphic, medium-grained
780.01	0.24	3.80E–04	9.20E–06	Granite to granodiorite, metamorphic, medium-grained
800.01	0.32	6.57E–04	1.15E–05	Granite to granodiorite, metamorphic, medium-grained
820.01	0.28	7.76E–04	1.10E–05	Granite, granodiorite and tonalite, metamorphic, fine- to medium-grained
840.17	0.10	9.28E–05		Granite, granodiorite and tonalite, metamorphic, fine- to medium-grained
860.01	0.16	2.78E–04	1.45E–05	Granite, granodiorite and tonalite, metamorphic, fine- to medium-grained, KFM01A
880.01	0.20	4.64E–04	8.93E–06	Granite to granodiorite, metamorphic, medium-grained

Borehole length (m)	Porosity (%)	Formation factor Lab	Formation factor In situ	Rock description
900.01	0.27	2.50E–04	1.47E–05	Pegmatite, pegmatitic granite, KFM01A
920.01	0.25	8.53E–04	1.36E–05	Granite to granodiorite, metamorphic, medium-grained
940.06	0.33	7.86E–04	1.57E–05	Granite to granodiorite, metamorphic, medium-grained
960.01	0.24	5.84E–04	1.44E–05	Granite to granodiorite, metamorphic, medium-grained
980.01	0.23	5.11E–04	1.09E–05	Granite to granodiorite, metamorphic, medium-grained
999.96	0.24	3.76E–04		Granite to granodiorite, metamorphic, medium-grained

Table A-4. Formation factor and porosity data from KFM02A.

Borehole length (m)	Porosity (%)	Formation factor Lab	Formation factor In situ	Rock description
101.01	0.20	9.33E–05		Granite to granodiorite, metamorphic, medium-grained,
121.01	0.36	1.47E–04		Granite to granodiorite, metamorphic, medium-grained
141.01	0.15	1.21E–04		Granite to granodiorite, metamorphic, medium-grained
161.01	0.21	1.60E–04		Granite, granodiorite and tonalite, metamorphic, fine- to medium-grained
201.01	0.10	7.19E–05	2.63E–05	Amphibolite
221.01	0.25	2.40E–04	2.93E–05	Granite to granodiorite, metamorphic, medium-grained
241.01	0.18	1.28E–04	2.27E–05	Granite to granodiorite, metamorphic, medium-grained
261.01	2.18	7.17E–04	2.66E–04	Granite to granodiorite, metamorphic, medium-grained
321.01	0.23	1.97E–04	4.63E–05	Granite to granodiorite, metamorphic, medium-grained
361.01	0.23	1.59E–04	2.19E–05	Granite to granodiorite, metamorphic, medium-grained
401.01	0.29	3.06E–04	2.93E–05	Granite to granodiorite, metamorphic, medium-grained
420.93	0.40	2.59E–04		Granite to granodiorite, metamorphic, medium-grained
440.96	0.18	1.00E–04	4.90E–05	Granite to granodiorite, metamorphic, medium-grained
460.96	0.38	3.46E–04		Granite to granodiorite, metamorphic, medium-grained
500.68	0.42	5.65E–04		Granite, granodiorite and tonalite, metamorphic, fine- to medium-grained
521.01	0.20	2.45E–04		Granite to granodiorite, metamorphic, medium-grained
541.01	0.25	1.52E–04		Granite to granodiorite, metamorphic, medium-grained
561.01	0.19	1.34E–04		Granite, granodiorite and tonalite, metamorphic, fine- to medium-grained
580.89	0.15	8.04E–05		Granite to granodiorite, metamorphic, medium-grained
601.01	0.21	1.44E–04	1.69E–05	Granite, granodiorite and tonalite, metamorphic, fine- to medium-grained
620.96	0.21	1.89E–04	2.03E–05	Granite to granodiorite, metamorphic, medium-grained
641.01	0.28	2.09E–04		Granite to granodiorite, metamorphic, medium-grained
661.01	0.22	2.05E–04	2.57E–05	Granite to granodiorite, metamorphic, medium-grained
681.01	0.19	2.01E–04	2.57E–05	Granite to granodiorite, metamorphic, medium-grained
701.01	0.25	2.91E–04	5.04E–05	Granite to granodiorite, metamorphic, medium-grained
721.01	0.22	3.48E–04	2.78E–05	Granite to granodiorite, metamorphic, medium-grained
741.01	0.20	2.90E–04	3.49E–05	Granite to granodiorite, metamorphic, medium-grained
761.01	0.22	2.63E–04	4.50E–05	Granite to granodiorite, metamorphic, medium-grained
781.01	0.23	3.64E–04	4.04E–05	Granite to granodiorite, metamorphic, medium-grained
801.01	0.27	3.63E–04	3.93E–05	Granite to granodiorite, metamorphic, medium-grained
821.01	0.24	3.77E–04	3.94E–05	Granite to granodiorite, metamorphic, medium-grained

Borehole length (m)	Porosity (%)	Formation factor		Rock description
		Lab	In situ	
841.01	0.27	3.70E–04	4.45E–05	Granite to granodiorite, metamorphic, medium-grained
861.01	0.30	6.74E–04	3.42E–05	Granite to granodiorite, metamorphic, medium-grained
881.01	0.25	4.66E–04	3.66E–05	Granite to granodiorite, metamorphic, medium-grained
901.01	0.22	3.30E–04	3.37E–05	Granite to granodiorite, metamorphic, medium-grained
921.01	0.15	1.44E–04	1.70E–05	Granite, granodiorite and tonalite, metamorphic, fine- to medium-grained
941.01	0.23	4.84E–04	2.31E–05	Granite to granodiorite, metamorphic, medium-grained
961.01	0.27	6.05E–04	2.71E–05	Granite to granodiorite, metamorphic, medium-grained
981.04	0.24	2.09E–04	2.85E–05	Granite to granodiorite, metamorphic, medium-grained
1001.01	0.25	3.76E–04		Granite to granodiorite, metamorphic, medium-grained